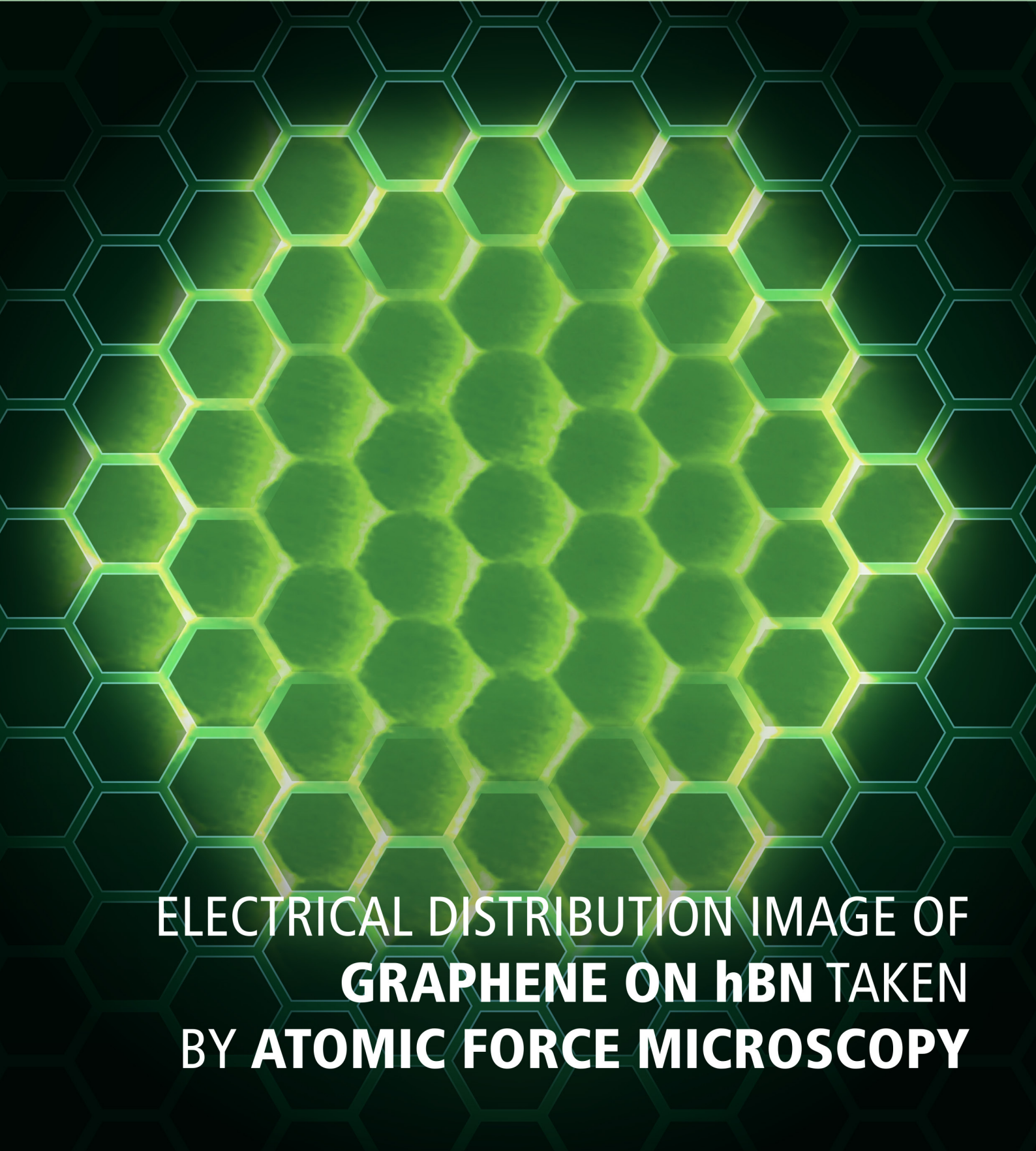


The Magazine for NANOsience and Technology

VOL 25 FALL-WINTER 2023

# NANOscientific



**ELECTRICAL DISTRIBUTION IMAGE OF  
GRAPHENE ON hBN TAKEN  
BY ATOMIC FORCE MICROSCOPY**



## 2023 NANOscientific Symposium Scanning Probe Microscopy (SPM)

# REGISTER NOW!

Join us for a truly international symposium on scanning probe microscopy! NANOscientific event will feature speakers from across the world, presenting groundbreaking research and discussing the latest advancements and techniques in SPM. Don't miss this opportunity to connect with the worldwide community of SPM researchers and expand your knowledge of this exciting field.

NANOscientific symposium brings together experts from around the globe to explore the science, engineering, and applications of nanotechnology. Featuring keynote addresses and virtual networking opportunities, attendees can form connections and propel their research, innovation, and businesses forward.



Sponsored By

NANOscientific

Park  
SYSTEMS

NWA  
NANOTECHNOLOGY  
WORLD ASSOCIATION

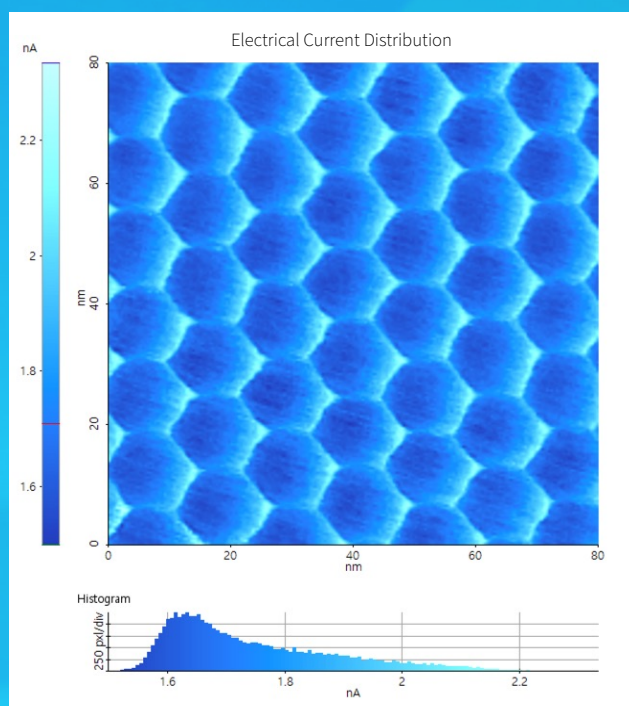
# ELECTRICAL CURRENT AFM IMAGE MAP OF GRAPHENE ON hBN IN NANOSCALE RESOLUTION

Hexagonal boron nitride (hBN), known in the scientific community as a wide bandgap semiconductor, stands out for its exceptional thermal and chemical stability. These characteristics make it indispensable in devices engineered to function under the most extreme conditions. In the realm of nanomaterials, hBN emerges as the perfect substrate for graphene. The two materials merge with minimal lattice mismatch, ensuring that graphene's superior carrier mobility remains uncompromised.

The AFM Current image captures a detailed area of 80 nm x 80 nm, vividly presenting the inherent hexagonal moiré structures of the sample. Each of these hexagons spans a width of 13 nm. Intriguingly, the electrical field becomes especially discernible at the lattice borders, registering a notable value of approximately 2.2 nA.

## Scanning Method:

This intricate image was captured using the Park Systems FX40. The Conductive AFM mode was employed during the scanning process using the SPARK 70 Pt probe (NuNano).



## INDEX

- Characterizing Displacement and Voltage Induced on a Piezo/Photodiode Device by Pulsed Laser Excitation Using Time-Resolved Kelvin Probe Force Microscopy** 4  
Andrea Cerreta et al.
- Intrinsic electrical characterization of two-dimensional transition metal dichalcogenides via scanning probe microscopy** 8  
Yuanyuan Shi et al.
- NanoScientific Magazine Interview** 11  
Professor Yuanyuan Shi, University of Science and Technology of China (USTC) Hefei, Anhui, China
- Advancing Electrical Characterization: Exploring the Capabilities of Scanning Microwave Impedance Microscopy Integrated with Atomic Force Microscopy** 13  
Armando Melgarejo, Park Systems, Inc., Nicholas Antoniou PrimeNano, Inc.
- Primer: Surface Analysis Techniques Using Atomic Force Microscopy** 15  
Chie Goto, Jong Deok Kim, Park Systems Japan
- NanoScientific Magazine Interview** 19  
Ranjith Ramadurai, Professor at Indian Institute of Technology Hyderabad, Medak, Telangana, India
- Dynamic self-stabilization in the electronic and nanomechanical properties of an organic polymer semiconductor** 21  
Illia Dobryden et al.
- News you might have missed...** 25

## NANOscientific

- **Keibock Lee**, Editor-in-Chief  
keibock@nanoscientific.org
- **Jessica Kang**, Managing Editor
- **Johnny Kim**, Editor and Point of Contact  
johnny@nanoscientific.org
- **Cathy Lee**, Technical Editor
- **Ester Cho**, Art Director

### Publisher and Corporate officers

- **Sang-il Park**, Chief Executive Officer
- **Karen Cho**, EVP of Finance
- **Ryan Yoo**: EVP of Business Development
- **Sang-Joon Cho**: EVP of Sales
- **Richard Lee**: EVP of Product Marketing

NanoScientific is published both in print and online to showcase advancements in the field of nanoscience and technology across a wide range of multidisciplinary areas of research. The publication is offered free to anyone who works or have interest in the field of nanotechnology, nanoscience, microscopy and other related fields of study and manufacturing.

We enjoy hearing from you, our readers. Please send your research or story ideas to [johnny@nanoscientific.org](mailto:johnny@nanoscientific.org).

To view all of our articles, please visit our web site at [magazine.nanoscientific.org](http://magazine.nanoscientific.org).

# CHARACTERIZING DISPLACEMENT AND VOLTAGE INDUCED ON A PIEZO/PHOTODIODE DEVICE BY PULSED LASER EXCITATION USING TIME-RESOLVED KELVIN PROBE FORCE MICROSCOPY

Andrea Cerreta<sup>1</sup>, Zeinab Eftekhari<sup>2</sup>, Rebecca Saive<sup>2</sup>, Alexander Klasen<sup>1</sup>

<sup>1</sup>Park Systems Europe, Germany

<sup>2</sup>Inorganic Materials Science, MESA+, University of Twente, Enschede, 7522NB, the Netherlands

## Introduction

Energy from different natural sources (light, wind, thermal, etc.) can be converted into measurable electrical quantities via a series of physical phenomena, some of which are at the basis of modern-day technologies. This application note specifically highlights piezo actuators and photodiodes as key devices where energy conversion plays a central role.

The piezoelectric effect describes the insurgence of a potential difference at two opposite sides of certain materials when a mechanical strain is applied to them. This is closely related to the fact that the deformation of the crystalline structure results into creation of dipoles at the unit cell level. Also, these materials display the reverse effect, where a mechanical deformation is observed when a voltage is applied to a piezoelectric sample. Piezoelectricity has a wide application in the fabrication of scanners and positioners.

Photodiodes are semiconductor devices primarily employed as light detectors due to their ability to generate a voltage proportional to the intensity of the incident light upon illumination of their surface. This working principle enables photodiodes to convert the amplitude, frequency, and phase of time-modulated light signals, such as sinusoidal or pulsed waves, into measurable electrical signals. Consequently, photodiodes find applications in wireless energy and information transfer.

By combining these two components, it is possible to create a device that integrates the following functions: 1) receiving a light signal as an input, 2) converting it into a voltage, and 3) triggering a mechanical displacement [1]. Devices that incorporate this scheme are referred to as piezo-photomotion devices.

The fabrication and characterization of these devices are among the primary focuses of Prof. Saive's research group in the Inorganic Materials Science (IMS) department at the University of Twente in the Netherlands. These applications hold potential in various fields, including micro/nanorobotics for biomedical purposes [2].

Atomic Force Microscopy (AFM) is an ideal technique for investigating the properties of piezo-photomotion devices. AFM exhibits sensitivity to sub-nanometer-scale topographic variations, enabling the detection of even the most subtle movements of these devices. Moreover, the AFM setup facilitates the application of Kelvin Probe Force Microscopy (KPFM), which provides valuable information regarding the surface potential and its variations in samples.

This application note is a result of the collaborative effort between Park Systems and IMS. The objective of this note is

to demonstrate how the Park Systems AFM (NX10), operating in KPFM mode, serves as a platform for comprehensive time- and position-dependent characterization of piezo-photomotion devices. The subsequent sections will provide details on the device structure, the experimental setup, and the results obtained from the KPFM experiments.

## Experimental

Exemplary devices were fabricated and characterized at IMS. These devices comprise a silicon photodiode integrated with lead zirconate titanate (PZT), a piezoelectric material represented by the blue layer in Figure 1a) [1]. The cross-section of the device reveals that the PZT actuator is positioned between lanthanum nickelate (LNO) electrodes on a 50  $\mu\text{m}$  silicon membrane, which forms the photosensitive component of the device.

The devices were placed in the Park NX10 microscope during the experiments. Illumination was provided by a light-emitting diode with a wavelength of about 630 nm, which is a part of the Photo Current Mapping (PCM) extension of the NX10 setup. The open design of the NX10's AFM head allows for ample space

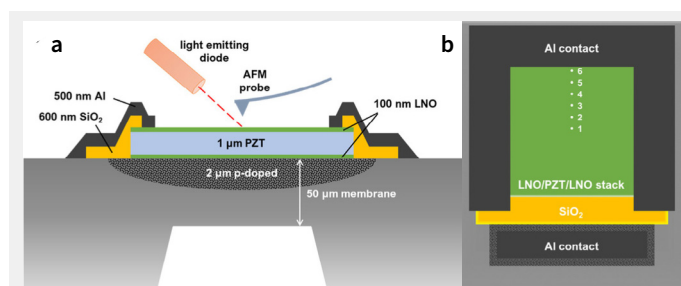


Figure 1. a) Sketch of the cross-section of the piezo-photomotion device. b) Top view of the device; the numbering indicates the positions on the active area of the sample where measurements were performed.

above the measurement area, providing flexibility in optimizing the angle and position of the impinging beam on the device's active area. Since the LNO/PZT/LNO stack is transparent in the spectral range of the diode, the light can reach the photodiode and hence generate a potential difference between the two electrodes, which leads to the deformation of the piezoelectric layer. Park AFMs are designed as sample scanners, meaning that the probe always remains stationary in the center of the tool, while the sample mounted on a XY scanner can be displaced laterally. Since the light-emitting diode and the AFM head are fixed with respect to the sample stage, only one initial alignment is needed to ensure the emitted beam illuminates the probed area of the sample.

The light source's on/off switching can be regulated using a triggering voltage. To achieve this, an external function generator (GW Instek SFG-1003) was connected to the emitter's triggering line, enabling alternate light switching on/off periods at a predetermined frequency. The emitter's rising time, which represents the time it takes to reach maximum power output, was evaluated to be less than 1  $\mu$ s.

Measurements were conducted in KPFM mode, which involves measuring the Contact Potential Difference (CPD) between the AFM probe and the sample at each position during imaging. Various approaches to implement KPFM exist, all of which rely on applying an oscillating electrical bias with a specific amplitude and frequency between the tip and the sample. This electrical excitation creates peaks in the vertical deflection spectrum of the cantilever, with amplitudes proportional to the CPD. By using a lock-in amplifier with this vertical deflection as an input signal, researchers can assess the amplitude at given frequencies and apply an additional potential that cancels out the CPD, effectively reducing the deconvoluted amplitude to zero. For more in-depth information on KPFM, please refer to [3]. In Sideband™ KPFM, the exciting bias frequency is chosen to produce peaks on the sidebands of the probe's mechanical resonance. As a result, peaks in that range are amplified, and the amplitude of these sidebands is more influenced by the tip-sample interaction than other forces acting on different parts of the cantilever [4]. This leads to a better quantitative and laterally resolved determination of the potential.

KPFM measurements can only be performed while scanning the sample in Dynamic (Tapping or Non-contact) mode. As a result, the system must be capable of deconvoluting both the amplitude of the resonant peak modulated by the sample's topography and the amplitude of electrically induced peaks modulated by the surface potential. To achieve this, the default Park Systems NX electronics are equipped with four independent lock-in amplifiers that can run in parallel, along with a feedback servo that acts on the tip DC bias. This setup allows for simultaneous mapping of both topography and potential without the need for a second pass at any scanned

line in lift mode, ensuring greater accuracy due to the closer distance of the tip to the sample. The Park Systems SmartScan™ software includes a built-in EFM/KPFM environment, enabling the effective and intuitive implementation of the Sideband KPFM mode.

## Results

The fabricated devices have an active area roughly in the shape of a square with sides measuring a few millimeters. For the initial test, the AFM probe was placed at the center of the membrane (position marked as 1 in Figure 1b). Since the main focus was to study the time dependence of the membrane response, the scanned area was reduced to a single point with zero lateral dimensions to limit topographic crosstalk, and signals were recorded over time. During Sideband KPFM experiments, an amplitude modulation-based feedback on the tip-sample distance was active, allowing tracking of any vertical changes in the surface position induced by the membrane movement in parallel to the potential shift. The results in Figure 2a show that when applying light excitation with a frequency of 1 Hz (0.5 seconds on, 0.5 seconds off), a vertical displacement of roughly 1 nm upwards was observed whenever the light was on. Additionally, under the same conditions, an increase in the surface potential of about 200 mV (difference between the top and bottom plateaux) was measured, demonstrating the basic principle of the device where the voltage generated by the photodiode through illumination is applied to the bottom electrode, causing the expansion of the piezoelectric stack. The 50 mV surface potential measured during the dark periods is attributed to the contact potential difference between the probe and the non-excited sample.

Additional tests were conducted at higher pulse frequencies, and the results for 2 and 4 Hz are shown in Figures 2b and c, respectively. Similar trends were observed, with the total displacement and photovoltage being noticeably smaller at 4 Hz. The plateau also becomes smaller at higher frequencies, and there is a more apparent transient time to reach the new status after light switching.

To further investigate the transient response time, photovoltage vs. time measurements were plotted together in Figure 3.

The photovoltage measured with a pulse frequency of 4 Hz is represented in red with a total time range of 1 second. Each pulse cycle's rising time ( $\tau$ ) spanning from the moment the light is switched on to when the plateau is reached is shown with a red background. The rising time was estimated to be about 80 msec, indicating a characteristic response feature of the device. While the photovoltage appears to reach a plateau for all the data plotted, the difference between the two levels when applying a 4 Hz pulse frequency appears slightly smaller than the other data. The exact reason for this effect is currently unclear, and further analysis is required to clarify this point. For now, we assume the value of 80 msec represents the qualitative behavior of the response as the correct rising time.

Photovoltage at pulse frequencies of 1 and 2 Hz were also plotted, with the signals conveniently shifted on the x-axis to have the light pulse start at the same time. Here,  $\tau$  is in good agreement among all the measurements. A model to describe the photo time response of the device is currently under development by IMS, and it has been hypothesized that it may be linked to the quality of the interface between the photodiode and the bottom electrode. The experiments presented here provide crucial information about the device's expected

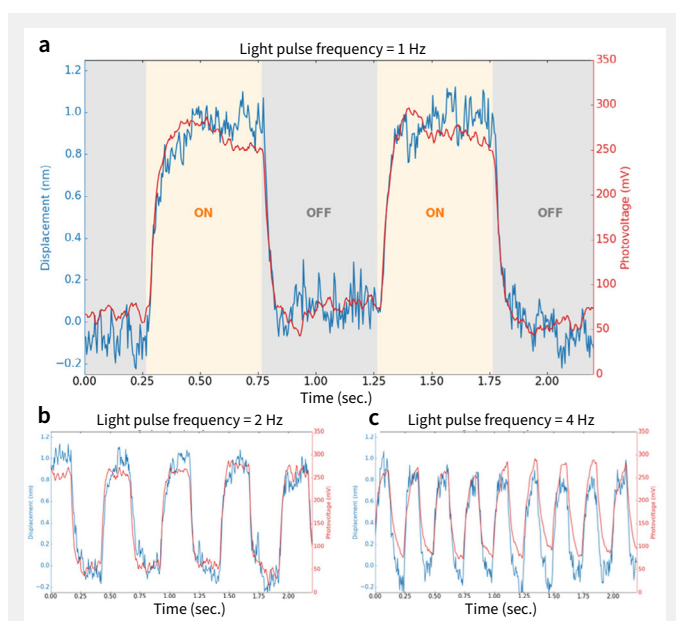


Figure 2: a) Comparison of the displacement and photo-induced voltage versus time with light pulsed at a switching frequency of 1 Hz. The device behaviors in time at frequencies equal to 2 Hz and 4 Hz are shown in b) and c) respectively.

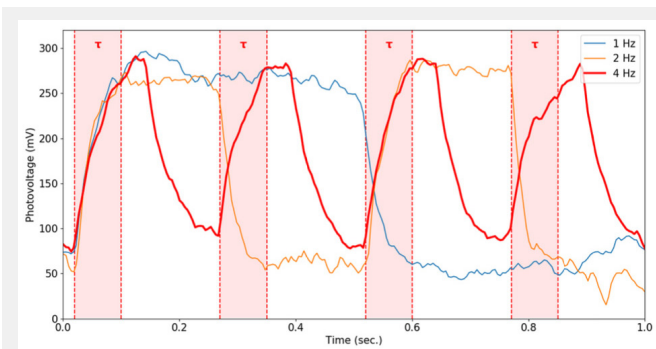


Figure 3. Photovoltage vs. time for light pulse frequency of 1, 2, and 4 Hz. The rising time of the photovoltage measured at 4 Hz is represented with a red background

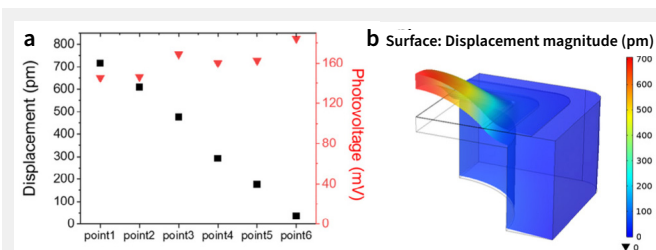


Figure 4. a) Mechanical displacement and surface potential at the positions indicated in Figure 1. b) 3D rendering of one quarter of the device, representing the vertical displacement of the PZT membrane.

performance at different communication rates with respect to the exciting light source and its efficiency in converting the transmitted signal into movement.

In a similar device, the AFM probe was approached in six different positions progressively farther distanced from the center and numbered as shown in Figure 1b. The objective was to measure the membrane's vertical displacement and light-induced photovoltage as a function of the position on the membrane. Light pulses with a frequency of 8 Hz were generated to excite the membrane. The results of this experiment are presented in Figure 4a.

It is observed that the displacement and photovoltage show different trends with respect to the position. The displacement reaches its maximum value at the center of the membrane (about 700 pm) and decreases to almost zero when reaching the side of the membrane. Notably, the displacement at the center is smaller than what was reported for the other device. This difference could be attributed to slight structural

variations among different devices or the fact that using an 8 Hz frequency results in a light on/off time of 62.5 msec, which is slightly lower than the estimated 80 msec rising time. Consequently, the higher pulse frequency may hinder the membrane from reaching the displacement plateau.

However, the photovoltage remained relatively constant at the different positions. This consistency might be attributed to the homogeneity of the silicon layer at the bottom of the device, ensuring a uniform photo-response throughout. Further simulations could provide additional insights into the underlying mechanisms and help substantiate interpretations of these observations. One hypothesis for the decreasing amplitude of the displacement with increasing distance from the center could be related to a mechanical restriction caused by the membrane's attachment to the sample support at its borders, resulting in reduced free oscillation.

## Conclusion

This application note demonstrates the working principle of piezo-photomotion devices. We showcase how AFM, particularly the setup and options provided by the Park Systems NX10 AFM, is the ideal choice for exploring the properties of such devices. We delve into KPFM measurements of the light-induced displacement and photovoltage as a function of time and position along the device membrane. The time response of the membrane expansion and voltage change is discussed, including the rising time from switch-off to switch-on status, providing an estimate of the membrane's maximum reaction rate to external light excitation at full efficiency. Furthermore, we analyze the dependence of the displacement on the position along the membrane, linking it to the mechanical constraints imposed by the device's geometry, as well as the homogeneity of the photovoltage response. These comprehensive measurements allow for the investigation and optimization of piezo-photomotion and other light-driven devices.

## References

- [1] W. M. Luiten, V. M. Van Der Werf, N. Raza, and R. Saive, "Investigation of the dynamic properties of on-chip coupled piezo/photodiodes by time-resolved atomic force and Kelvin probe microscopy," *AIP Adv.*, vol. 10, no. 10, Oct. 2020, DOI: 10.1063/5.0028481.
- [2] Z. Zhan, F. Wei, J. Zheng, W. Yang, J. Luo, and L. Yao, "Recent advances of light-driven micro/nanomotors: Toward powerful thrust and precise control," *Nanotechnol. Rev.*, vol. 7, no. 6, pp. 555–581, 2018, DOI: 10.1515/ntrev-2018-0106.
- [3] A. Axt, I. M. Hermes, V. W. Bergmann, N. Tausendpfund, and S. A. L. Weber, "Know your full potential: Quantitative Kelvin probe force microscopy on nanoscale electrical devices," *Beilstein J. Nanotechnol.*, vol. 9, 1809–1819, 2018, DOI: <https://doi.org/10.3762/bjnano.9.172>
- [4] J. Colchero, A. Gil, and A. M. Baro, "Resolution enhancement and improved data interpretation in electrostatic force microscopy," *Phys. Rev. B*, vol. 64, 245403, 2001, DOI: 10.1103/PhysRevB.64.245403

# One Nanostep for Microscopy One Giant Leap for Science



## Park FX40

A New Class of Atomic Force Microscope: The Automatic AFM

The Park FX40 autonomously images and acquires data powered by its artificial intelligence, robotics and machine learning capability. Effortlessly, get the sharpest, clearest, highest resolution images and measurements one sample after another on various applications. Boost your progress and scientific discoveries through unprecedented speed and accuracy.



More Information

# INTRINSIC ELECTRICAL CHARACTERIZATION OF TWO-DIMENSIONAL TRANSITION METAL DICALCOGENIDES VIA SCANNING PROBE MICROSCOPY

Yuanyuan Shi<sup>1</sup>, Jill Serron<sup>1</sup>, Benjamin Groven<sup>1</sup>, Albert Minj<sup>1</sup>, Pierre Morin<sup>1</sup> and Thomas Hantschel<sup>1</sup>  
<sup>1</sup>IMEC, Kapeldreef 75, 3001 Leuven, Belgium

The following application note is based on ACS Nano publication, 2021 15, 6, 9482–9494.

## Introduction

In a conventional planar silicon field effect transistor (FET), the gate controllability becomes weaker when its lateral dimension becomes smaller than the transistor thickness, which results in adverse short-channel effects, including leakage current, saturation of the carrier mobility in the channel, channel hot-carrier degradation, and time-dependent dielectric breakdown. Hence, the transistor body thickness needs to be reduced to ensure efficient electrostatic control from the gate. Due to the atomic thickness and dangling bond-free surface of two-dimensional (2D) materials, theoretical studies have shown that particularly 2D transition metal dichalcogenides (TMDs) can outperform Si as the channel material, enable the atomic-level scaling, excellent electrostatic gate control, decrease off-state power consumption and further extend Moore's Law.<sup>[1–6]</sup>

Suitable techniques to characterize the intrinsic physical and electrical properties of as-deposited 2D materials, are a key link between the quality of as-deposited 2D materials and the performance of 2D materials-based electronic devices. This link can help us to better understand, control and improve the performance of 2D materials-based devices. However, techniques for analyzing the intrinsic electrical properties of as-deposited 2D materials on the nanoscale without any transfer and patterning process are limited.

In this application note, scanning probe microscopy (SPM) is used to investigate the intrinsic electrical properties of as-deposited 2D TMDs. Conductive atomic force microscope (C-AFM) is performed directly on the surface of as-grown 2D materials without any patterning. C-AFM allows correlating the electrical conductivity of as-grown 2D materials to their topography, thereby linking the electrical properties of 2D materials to their physical properties such as layer thickness, etc. With all of this, C-AFM gives us comprehensive information of as-deposited 2D materials and helps us to evaluate the impact of these intrinsic properties on 2D materials-based nanoelectronics.

## Experimental Details

The intrinsic electrical properties of the as-grown MoS<sub>2</sub> and WS<sub>2</sub> layers on sapphire are evaluated by C-AFM using Pt/Ir coated Si probes (spring constant  $k \sim 3$  N/m, resonance frequency  $f_0 \sim 75$  kHz, PPP-EFM) on a Park NX-Hivac AFM under high vacuum ( $\sim 10^{-5}$  Torr). The high vacuum environment can help to reduce the water layer which always exists on the sample.<sup>[4,6]</sup> The bias of the C-AFM measurement is applied to the sample chuck and the resulting current is measured through a linear current amplifier. The applied bias to collect all the C-AFM current maps is all at 1 V. Electrical contact is ensured by applying silver paint to the top and side of the samples.

## Results and Discussion

The as-deposited MoS<sub>2</sub> layer on on-axis cut sapphire displays a non-uniform conductance over the whole surface in the C-AFM current maps (Figure 1b), even though the topography maps in Figure 1a show a fully coalesced monolayer MoS<sub>2</sub> with  $\sim 37\%$  superficial crystals on top of it (named as 1.3 ML). By introducing the off-axis 1° cut sapphire as substrate, the electrical conductivity of the MoS<sub>2</sub> layer becomes more homogeneous in line with their more uniform surface structure (Figure 1c and d). Overall, a fraction of  $\sim 83\%$  of monolayer MoS<sub>2</sub> on off-axis 1° cut sapphire possesses a higher electrical conductivity, as compared

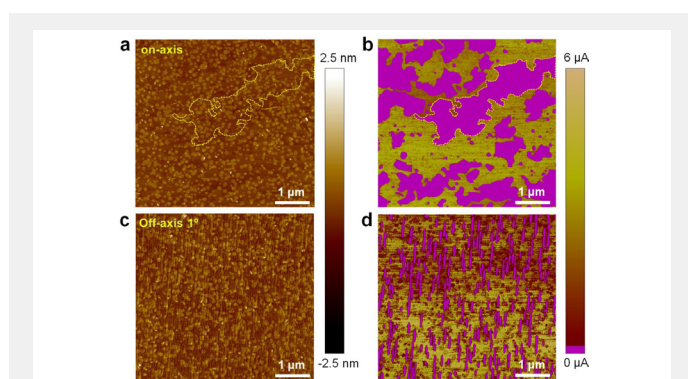


Figure 1. (a, c) C-AFM topography of 1.3 ML MoS<sub>2</sub> grown on on-axis and off-axis 1° cut sapphire, respectively. (b, d) The simultaneously acquired C-AFM current maps of (a, c), respectively. Non-homogeneous and poorly conductive regions in the first single layer of MoS<sub>2</sub> are highlighted in pink by current thresholding ( $\sim 0.3 \mu\text{A}$ ). Images are reproduced with permission.<sup>[7]</sup> Copyright 2021, American Chemical Society.

to only 51% using on-axis cut sapphire.[7] The regions with lower conductivity are marked in pink in Figure 1b, d with a threshold current of  $\sim 0.3 \mu\text{A}$ . Thus, the density of poorly conductive regions is reduced by introducing the off-axis  $1^\circ$  cut sapphire (from 49% to 17% in Figure 1b, d).

This density can be further reduced to  $\sim 6.5\%$  by skipping the pre-epi treatment process of the sapphire wafers (Figure 2a-b). The shapes of the  $\text{MoS}_2$  regions with lower conductivity are not random, but correspond to the specific underlying sapphire terraces. The regions with lower  $\text{MoS}_2$  conductivity on off-axis  $1^\circ$  cut sapphire correspond to the terraces that have bunched together. During the pre-epi treatment and Metal organic chemical vapor deposition (MOCVD) process, steps decompose and agglomerate. Step (de-)formation is primarily driven by the high temperatures used in both pre-epi treatment and MOCVD process. Step bunching becomes more probable as  $W_{\text{terrace}}$  narrows, as expected for off-axis  $1^\circ$  cut sapphire. When the monolayer  $\text{MoS}_2$  is deposited on off-axis  $1^\circ$  cut sapphire without any pre-epi treatment, the density of highly conductive regions increases further from 83% (Figure 1d) to 93.5% (Figure 2b). A clear correlation can be observed between the bunched steps (with a higher  $H_{\text{terrace}}$ , 5.8% in Figure 2a) and poorly conductive regions (6.5% dark regions in Figure 2b). The extracted cross-sectional profiles from the topography and current maps in Figure 2c further support this observation. However, the poorly conductive regions are not completely removed in Figure 2b. This should be related to the growth temperature ( $1000^\circ\text{C}$  in our work), which is high enough to introduce step bunching on the sapphire surface during the deposition.[8-10]

Regarding the observed inhomogeneity of the  $\text{MoS}_2$  conductivity distribution, we found that the presence of  $\text{MoS}_2$  crystals in the non-closed top layers does not influence the conductivity. Indeed,  $\text{MoS}_2$  regions with lower conductivity remain nearly constant with  $\text{MoS}_2$  layer thickness, since they also exist in the Figure 2a) and poorly conductive regions (6.5% dark regions in Figure 2b). The extracted cross-sectional profiles from the topography and current maps in Figure 2c further support this 3.5 ML  $\text{MoS}_2$  (Figure 2d-e): A comparison of the dashed yellow outlined regions in topography and current image shows that  $\text{MoS}_2$  crystals with a misoriented basal plane in the non-closed top layers do not influence the conductivity in that region. Moreover, it is worth to note that the existence of regions with different conductance not only occurs in the  $\text{MoS}_2$  epitaxial layer, but also in the MOCVD  $\text{WS}_2$  layer grown on sapphire, as shown in Figure 3.

Thus, the lower conductivity relates primarily to the fully closed first  $\text{MoS}_2$  single layer rather than the non-closed top layers. Figure 4a-b further supports this by showing two 2nd layer  $\text{MoS}_2$  crystals with some regions of higher conductivity and some regions of lower conductivity.

The results indicate that the state of the sapphire starting surface is one of the key parameters determining the physical and electrical properties of the first  $\text{MoS}_2$  single layer.

## Conclusions

The intrinsic electrical properties of 2D TMDs are evaluated via C-AFM and linked to the sample topography. We found a non-homogenous conductivity in the as-deposited 2D TMDs single layer, which possibly originates from: (i) TMDs surface

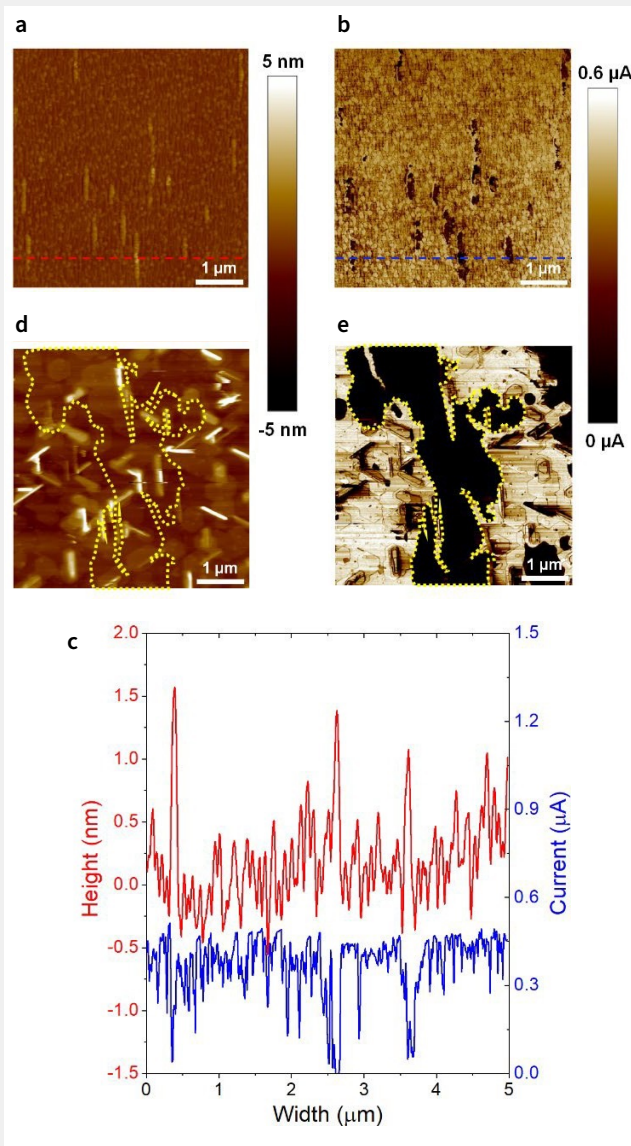


Figure 2. Inhomogeneous electrical conductivity of  $\text{MoS}_2$  grown on sapphire. (a-b) C-AFM topography and simultaneously obtained current map of 1.3 ML  $\text{MoS}_2$  on as-received off-axis  $1^\circ$  cut sapphire. (c) Corresponding cross-sectional height (red) and current (blue) profiles at the positions in (a-b), respectively. (d-e) Topography and simultaneously obtained current map of 3.5 ML  $\text{MoS}_2$  on on-axis cut sapphire. Images are adapted with permission from Ref. [7]. Copyright 2021, American Chemical Society.

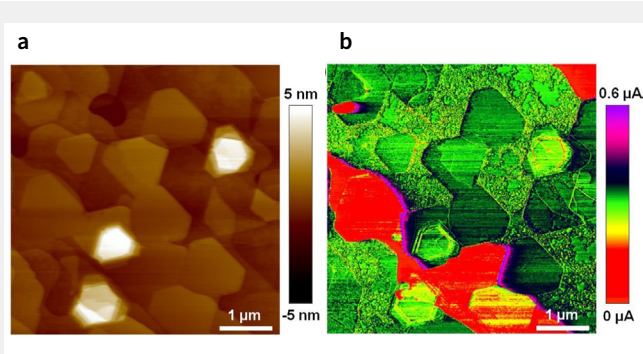


Figure 3. (a-b) Topography and simultaneously obtained current map of 1.7 ML  $\text{WS}_2$  on on-axis cut sapphire. Images are adapted with permission from Ref. [7]. Copyright 2021, American Chemical Society

roughness from TMDs layer thickness variation; (ii) TMDs strain induced by sapphire surface topography; (iii) TMDs intra-grain defectivity due to dependence of TMDs nucleation rate per sapphire terrace; or (iv) TMDs interface defectivity induced by sapphire surface structure and termination, which could result in differently local doping effects. Further investigation is in process to combine C-AFM with advanced spectroscopy techniques (such as Raman, PL and TOFSIMS) to further explore the intrinsic properties of the epitaxial 2D materials.

## References

- (1) Liu, Y.; Duan, X.; Shin H.-J.; Park, S.; Huang, Y.; Duan, X. Promises and Prospects of Two-Dimensional Transistors. *Nature* 2021, 591, 43–53.
- (2) Su, S.-K.; Chuu, C.-P.; Li, M.-Y.; Cheng, C.-C.; Wong, H.-S. P.; Li, L.-J. Layered Semiconducting 2D Materials for Future Transistor Applications. *Small Struct.* 2021, 2, 2000103.
- (3) Akinwande, D.; Huyghebaert, C.; Wang, C.-H.; Serna, M. I.; Goossens, S.; Li, L.-J.; Wong, H.-S. P.; Koppens, F. H. L. Graphene and Two-Dimensional Materials for Silicon Technology. *Nature* 2019, 573, 507–518.
- (4) Agarwal, T.; Szabo, A.; Bardon, M. G.; Soree, B.; Radu, I.; Raghavan, P.; Luisier, M.; Dehaene, W.; Heyns, M. Benchmarking of Monolithic 3D Integrated MX2 FETs with Si FinFETs. In 2017 IEEE International Electron Devices Meeting (IEDM); 2017; p 5.7.1–5.7.4.
- (5) Smets, Q.; Arutchelvan, G.; Jussot, J.; Verreck, D.; Asselberghs, I.; Nalin Mehta, A.; Gaur, A.; Lin, D.; Kazzi, S. E.; Groven, B.; Caymax, M.; Radu, I. Ultra-Scaled MOCVD MoS<sub>2</sub> MOSFETs with 42nm Contact Pitch and 250 $\mu$ A/mm Drain Current. In 2019 IEEE International Electron Devices Meeting (IEDM); 2019; p 23.2.1–23.2.4.
- (6) Smets, Q.; Verreck, D.; Shi, Y.; Arutchelvan, G.; Groven, B.; Wu, X.; Sutar, S.; Banerjee, S.; Nalin Mehta, A.; Lin, D.; Asselberghs, I.; Radu, I. Sources of variability in scaled MoS<sub>2</sub> FETs. In 2020 IEEE International Electron Devices Meeting (IEDM); 2020; p 3.1.1–3.1.4.
- (7) Shi, Y.; Groven, B.; Serron, J.; Wu, X.; Nalin Mehta, A.; Minj, A.; Sergeant, S.; Han, H.; Asselberghs, I.; Lin, D.; Brems, S.; Huyghebaert, C.; Morin, P.; Radu, I.; Caymax, M. Engineering Wafer-Scale Epitaxial Two-Dimensional Materials through Sapphire Template Screening for Advanced High-Performance Nanoelectronics. *ACS Nano* 2020, DOI: 10.1021/acsnano.0c07761.
- (8) Cuccureddu, F.; Murphy, S.; Shvets, I. V.; Porcu, M.; Zandbergen, H. W.; Sidorov, N. S.; Bozhko, S. I. Surface Morphology of C-Plane Sapphire ( $\alpha$ -Alumina) Produced by High Temperature Anneal. *Surf. Sci.* 2010, 604, 12941299.
- (9) Curio, S.; Chatain, D. Surface Morphology and Composition of C-, a- and m-Sapphire Surfaces in O<sub>2</sub> and H<sub>2</sub> Environments. *Surf. Sci.* 2009, 603, 2688–2697.
- (10) Ribiq, P. R.; Bratina, G. Behavior of the (0001) Surface of Sapphire upon High-Temperature Annealing. *Surf. Sci.* 2007, 601, 44–49.

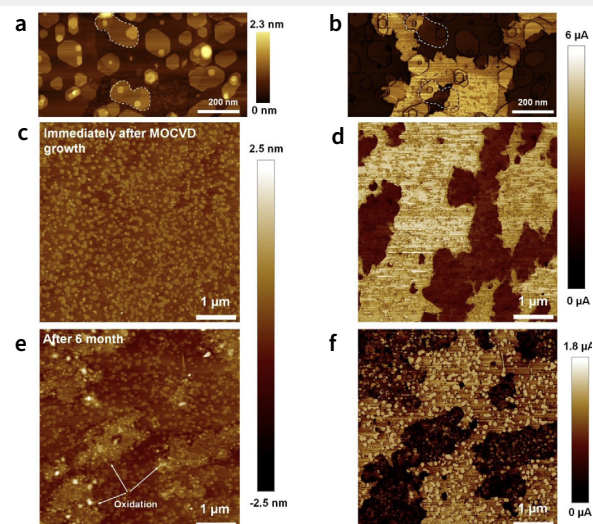


Figure 4. (a-b) Electrical conductivity of 2nd-3rd layer MoS<sub>2</sub> islands on the 1.3 ML MoS<sub>2</sub> grown on on-axis cut sapphire. (a) Topography and its corresponding (b) current map of the MoS<sub>2</sub> grown on on-axis cut sapphire. The white color outlines crystals show partial regions with higher conductivity and partial regions with lower conductivity, indicating that the superficial crystals do not contribute much to the inhomogeneous conductivity of the MoS<sub>2</sub> on sapphire. (c-f) Degradation of 1.3 ML MoS<sub>2</sub> grown on on-axis cut sapphire. (c-d) Topography and its corresponding current map at 1 V of the 1.3 ML MoS<sub>2</sub> collected immediately after the MOCVD growth. (e-f) Topography and current map at 1 V of the same sample after 6 months storage in a N<sub>2</sub> cabinet. No oxidized regions in (c), but the MoS<sub>2</sub> are partially oxidized in (e), which always correlates to the poorly conductive regions in (f). Images are adapted with permission from Ref. [7]. Copyright 2021, American Chemical Society.

# Ideal for **Failure Analysis** and **Sensitive Materials Research**



## Park **NX-Hivac**

Park NX-Hivac allows failure analysis engineers to improve the sensitivity and repeatability of their AFM measurements through high vacuum environment. Because high vacuum measurement offers greater accuracy, better repeatability, and less tip and sample damage than ambient or dry N2 conditions, users can measure a wider range of signal response in various failure analysis applications.



More Information

# NANOSCIENTIFIC MAGAZINE INTERVIEW

Professor Yuanyuan Shi  
University of Science and Technology of China (USTC)  
Hefei, Anhui, China

## About the Professor

Professor Yuanyuan Shi is a researcher in the field of nanoscience and nanotechnology, known for her groundbreaking contributions to the development of novel nanoelectronic devices. Currently serving as a professor at the University of Science and Technology of China (USTC), Professor Shi leads the “Integrated Nanoelectronics and X-computing (iNext) lab,” where her research primarily focuses on the integration of innovative thin-film transistors for logic, memory, and brain-inspired computing applications. Before joining USTC, she was a senior researcher at IMEC, Belgium. She conducted research on emerging non-volatile memories, thin film growth and characterization, nanoelectronics (especially scaled MOSFETs) fabrication, device physics, and neuromorphic computing. Her remarkable achievements include publishing over 70 research articles in prestigious journals/conferences, receiving IEEE EDS PhD award, Marie Curie fellowship and earning recognition as a Forbes “30 under 30” recipient. Professor Shi’s extensive experience in both academia and industry, is advancing nanotechnology research, shaping the future of electronics and computing. Her contributions inspire the next generation of researchers in nanoelectronics.



## About the University

The University of Science and Technology of China (USTC) in Hefei, Anhui, has been a renowned academic and research institution since its founding in 1958. It excels in physics, engineering, and computer science, producing influential scientists. USTC’s focus on cutting-edge research attracts global talents and contributes significantly to scientific knowledge.

USTC is among the leading universities in Chinese nanoscience and nanotechnology, with the Hefei National Laboratory for Physical Sciences at the Microscale (HFNL) at the forefront. Equipped with advanced facilities, including Atomic Force Microscopy (AFM), USTC conducts pioneering research in nanomaterials and devices for energy, electronics, and medicine.



**NS:** Could you share some insights into your current research at the “Integrated Nanoelectronics and X-computing (iNext) lab”? What are the main goals and objectives of your research team?

**Shi:**

*In iNext lab, we focus on exploring the design, integration processes, and device physics of thin-film transistors based on 2D semiconductors and oxide semiconductors, along with their applications in high-performance logic, memory, and brain-inspired computing devices. We anticipate that our research will offer new opportunities for CMOS logic scaling at advanced technology nodes, as well as novel memory architectures and computing paradigms.*

**NS:** In your work, you mention focusing on materials, concepts, and architectures for logic and memory devices. Can you elaborate on some of the novel materials or concepts you find particularly promising for future electronic devices?

**Shi:**

*Yes, I would like to give two-dimensional (2D) semiconductors as an example here for CMOS logic scaling. Abundant-data computing such as big-data analytics, artificial intelligence (AI) and Internet of Things (IoT) demand extreme energy efficiency and concomitant improvement of cost performance of the electronic systems. Silicon-based field-effect transistors (FETs) are the fundamental building blocks of modern computing microprocessors. Following Moore’s law, an exponentially increasing number of transistors is integrated into a computing microprocessor, enabled by the scaling of silicon transistors. This makes modern chips faster, more powerful, and cost-effective. Nowadays, the scaling of silicon transistors faces increased technical challenges, such as short-channel effects, making the exploration of alternative new channel materials and device geometries even more crucial for future computing chips. Atomically thin 2D semiconductors is a new kind of channel materials that could facilitate continued transistor scaling, meeting the power, performance, area, cost (PPAC) demands of future electronic devices.*

**NS:** You’ve published numerous research articles in prestigious journals/conferences like Nature Electronics, ACS Nano, and IEDM. Can you highlight a few key findings or breakthroughs from your research that you’re particularly proud of?

**Shi:**

*Yes, I would like to give the key finding in my IEDM paper (2021) as an example. The motivation of this study was the theoretical prediction of ultimate scaling of CMOS logic transistors with atomically thin (monolayer) 2D semiconductors as channel material. However, the uniform monolayer deposition of 2D semiconductors at wafer scale is still challenging. In our IEDM paper (2021), we provided a novel deposition concept for in-situ deposition and etching of 2D semiconductors and obtained the uniform monolayer MoS<sub>2</sub> film at wafer scale. Furthermore, the scaled transistors with*

this uniform monolayer MoS<sub>2</sub> as channel statistically showed better performance, especially for V<sub>th</sub> variation (on par with advanced Si FinFETs) and inhibition to short channel effects, compared to nonuniform monolayer MoS<sub>2</sub> based transistors. This work demonstrates the superior electrostatic of atomically thin 2D semiconductors-based transistors and their potential for ultimate transistor scaling.

**NS:** You've had the opportunity to work in both academic and industry research settings. How do these experiences differ, and how have they shaped your approach to nanoscience research?

**Shi:**

Over my experience in academia and industry, research in academia provides more freedom to pursue the demonstration of new concepts/ideas and a deep understanding of device physics, among other aspects. Meanwhile, the industry, with its industrial infrastructure, can be more beneficial for addressing engineering questions, such as pilot-line process integration, the transition from lab to fab, and industrialization.

**NS:** Could you tell us more about your work on thin-film transistors (TFTs) and their potential applications in logic, memory, and brain-inspired computing? What role do 2D semiconductors and metal oxides play in your research?

**Shi:**

In my group, we are exploring thin-film transistors based on two kinds of channel materials: 2D semiconductors and oxide semiconductors. Both of them face similar problems, such as high-quality channel deposition, defect-free modulation,

interface engineering, contact resistance, and CMOS integration, among others. The requirements for device performance differ for logic, memory, and brain-inspired computing applications. Typically, logic transistors require scaling capability, high mobility, and inhibition of short-channel effects, among other factors. For memory applications, specifically capacitorless DRAM, one of the main challenges is the trade-off between threshold voltage and on-current for thin-film transistors-based capacitorless DRAM technology. Devices for brain-inspired computing are more tolerant of stochasticity, mobility, subthreshold swing, and other factors.

**NS:** How do you see nanoelectronics and nanotechnology contributing to the development of next generation computing technologies, including quantum computing and neuromorphic computing?

**Shi:**

Nowadays, digital computing is increasingly capacity-limited and power-limited, which is determined by the slowing down of transistor scaling and the exponential growth of computing needs. This drives most research in nanoelectronics and nanotechnology. Since around 2006, the need for shrinking devices, the bottleneck of the von Neumann computing paradigm, and the limitations of digital information processing have made society realize the urgency of new computing paradigms. One of the promising approaches is to perform computing based on intrinsic nanoelectronics device dynamics, so that each device functionally replaces elaborate digital circuits, leading to adaptive complex computing.

## Active Vibration Isolation System

# The Ultimate Stability and Accuracy Solution for your Scientific Research



## Accurion i4

- Unmatched stability and precision with dynamic vibration isolation in six degrees of freedom.
- Fast settling time of 0.3 seconds or under with auto load adjustment and transport lock.
- Advanced active vibration isolation system with instant counterforce for maximum precision.
- Versatile vibration isolation.

# ADVANCING ELECTRICAL CHARACTERIZATION: EXPLORING THE CAPABILITIES OF SCANNING MICROWAVE IMPEDANCE MICROSCOPY INTEGRATED WITH ATOMIC FORCE MICROSCOPY

Armando Melgarejo, Park Systems, Inc., Nicholas Antoniou PrimeNano, Inc.

## Introduction

The understanding of electrical properties in materials is a growing concern in materials research and the semiconductor industry. To address the limitations of current methods, new and existing technologies are being adapted. This technical note introduces ScanWave Scanning Microwave Impedance Microscopy (sMIM) as a new imaging mode for Park Systems Atomic Force Microscopes (Park AFMs). sMIM utilizes microwave reflections from the tip-sample interaction to gather local electrical properties, including permittivity, conductivity, dielectric constant, capacitance, resistivity, and dopant concentration (for semiconductors) at the nanoscale (Figure 1). This knowledge is crucial for maintaining high-quality and reliable processing of materials like semiconductors, thin films, and dielectrics.

ScanWave provides significant advantages compared to other electrical AFM modes, for the following reasons:

- sMIM is based on a microwave signal, minimizing or eliminating the need for sample preparation.
- No path to ground through the

sample is required, as there is no current flow involved.

- Floating insulators and dielectrics can be directly imaged without difficulty.

sMIM offers a log-linear response to capacitance/dielectric constant and dopant level (Figure 2), simplifying quantification. In comparison to SCM (Scanning Capacitance Microscopy), sMIM offers several additional capabilities including measurements of DC capacitance, DC resistance, as well as dC/dV and dR/dV. On the other hand, SCM only provides measurements of dC/dV, which is much harder to quantify compared to sMIM measurements.

Furthermore, both SSRM (Scanning Spreading Resistance Microscopy) and SCM require extensive sample preparation and setup. Moreover, ScanWave Pro boasts a capacitance sensitivity of 0.075 aF, enabling the imaging of even minute variations in capacitance, resistance, and dopant levels down to intrinsic silicon (refer to Figure 2). Capacitance vs. Voltage (C-V) is a widely used measurement technique for semiconductors, and by sweeping a DC voltage on the probe, C-V measurements can be obtained with nanoscale positioning.

By utilizing ScanWave sMIM module from PrimeNano on Park AFMs, high-quality images of variations in conductivity and permittivity can be obtained [1]. The combination of AFM and sMIM enables simultaneous measurements across various channels: capacitance variations, resistance variations, dC/dV amplitude and phase, dR/dV amplitude and phase and surface topography (other concurrent mechanical information is also available). In semiconductors, dopant carrier concentration and type are found through a reference sample.

Moreover, Park AFM offers beyond the combination of Non-contact mode imaging, which eliminates sample damage, by enhancing sMIM with the integration of PinPoint [2] and QuickStep [3] technology. These advanced sMIM techniques not only allow high-quality electrical characterization of challenging samples but also provide the following advantages:

- Elimination of shearing forces associated with contact-based electrical modes, which can lead to scanning artifacts and sample damage.
- Reduction in tip wear, resulting in a sharper tip for an extended period.
- Facilitation of correlative microscopy through multichannel measurements, allowing simultaneous acquisition of electrical properties and nanomechanical properties such as Young's modulus.

Furthermore, PrimeNano provides ScanWave Pro Solutions [4], an automated technique specifically designed for precise quantification of dopant measurements. It offers a remarkable dopant spatial resolution of 10 nm, with a repeatability better than 0.1 of a decade of dopant level.

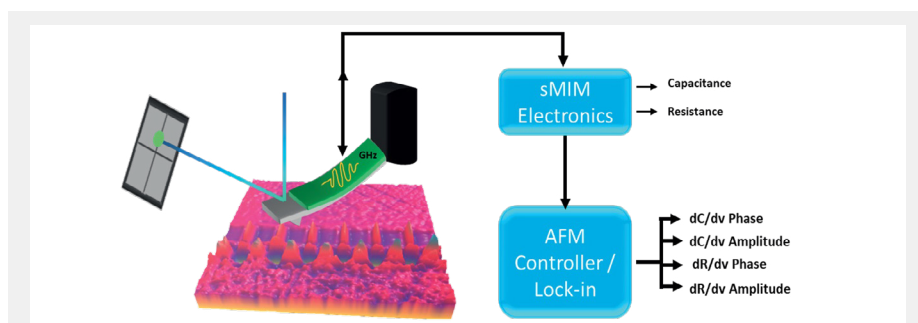


Figure 1. Diagram of the fundamentals of sMIM. The microwave signal is transmitted via the shielded probe to the tip where it interacts with the sample. The reflected waves are collected and transmitted back to ScanWave electronics where they are demodulated into relative capacitance and resistance. By adding an AC signal on top of the microwaves and using a lock-in amplifier, properties such as phase and amplitude for dC/dV or dR/dV can be measured.

## Experimental

The sMIM imaging is supported by all existing Park AFM research systems. The interface to collect microwave signals and generate AFM images is provided by SmartScan [5] and ScanWave [1]. It is necessary to use commercially available cantilevers that have a shielded signal path to the tip. The operational scheme, including the mounting of the tip, creation of the near-field electromagnetic wave at the tip, and generation of the final image, can be completed in four simple steps:

1. Mount the tip and sample, and align the beam-bounce system using SmartScan's guided mode.
2. Utilize the Auto mode on SmartScan to bring the tip and sample into close proximity.
3. Wait. ScanWave generates microwaves that interact with the sample through a shielded probe, creating a localized electromagnetic wave at the tip's apex. The resulting microwave signal is demodulated by the ScanWave software automatically.
4. Initiate AFM scanning and data acquisition, allowing the user to manually select scan parameters or rely on SmartScan's automated selection.

## Result

All images from SRAM sample shown in Figure 3 were acquired simultaneously. Data depicts only a section of two SRAM cells, NMOS transistors shown. Figures 3.b and 3.c are the phase and amplitude of the dC/dV channel, respectively. The dC/dV phase (Figure 3.b) reveals that the SRAM sample primarily consists of N-dopant, the pink areas corresponding to the source/drain regions, while P-dopant is present in the channel (the black regions). The dC/dV amplitude illustrates variations in dopant concentration across the sample, with the white regions/implants representing areas within the channel that have lower doping levels compared to the source/drain areas.

For the reference sample shown in Figure 4, the goal was to measure the capacitance across it. Figure 4.b illustrates the variations in capacitance across the sample, which correspond to the relative levels of dopant concentration. The reference standard consists of stepped regions, with increasing N-type dopant concentration from the left side to the center and decreasing p-type dopant concentration from the center to the right edge. By scanning the reference sample, the sensitivity of the technique can be verified, and the phase signal can be demodulated to separate and measure the capacitance and resistance channels. Furthermore, it establishes a reference value that enables subsequent quantification of the measured data.

## Conclusion

This technical note provides an overview of the capabilities of Scanning Microwave Impedance Microscopy in obtaining high-quality electrical property data from a wide range of samples. The integration of ScanWave with Park AFMs establishes a powerful characterization tool for the development and quality control of semiconductor manufacturing processes, including dopant incorporation and dielectric film formation. Furthermore, sMIM holds potential for additional nanoelectrical characterization in various areas such as semiconductors, dielectrics, metal oxides, ferroelectrics, and 1D and 2D materials.

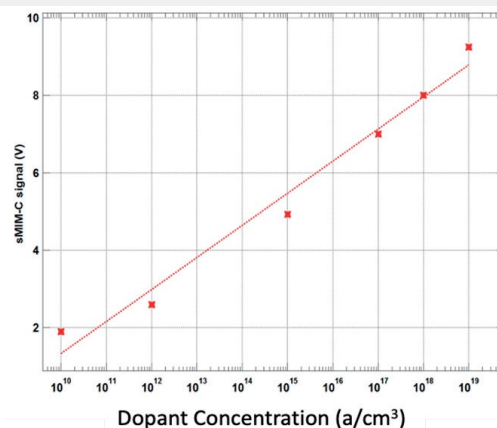


Figure 2. ScanWave Response to Dopant Concentration.

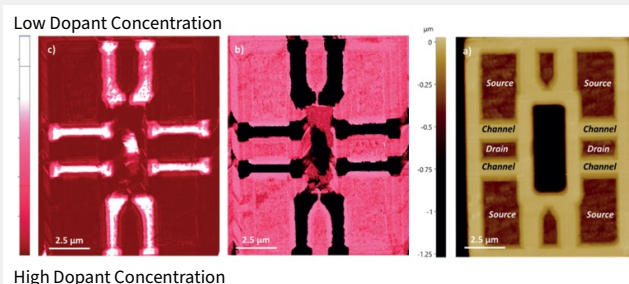


Figure 3 showcases the Static Random Access Memory (SRAM), highlighting the N-type metal oxide semiconductor (NMOS) implant in the results. Images: (a) Topography image displaying a subunit of the memory. (b) dc/dv phase image, where the contrast represents the dopant type. The selected implant consists primarily of N-dopant structures, indicated by the pink areas. (c) dc/dv amplitude image, which reveals the dopant concentration. The red areas exhibit a lower dopant concentration compared to the white regions within the NMOS.

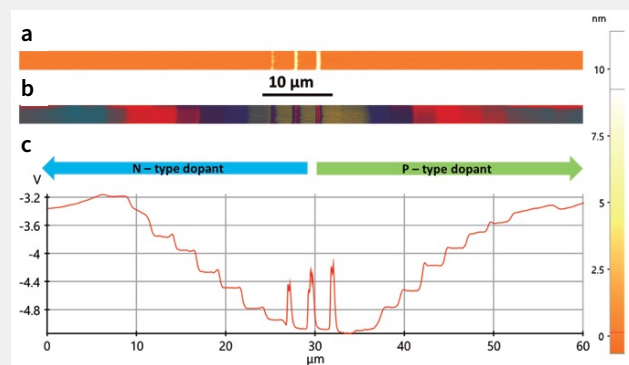


Figure 4 displays a reference sample with dopant implants, featuring a staircase of P and N doped regions. Images: (a) Topography image. (b) Capacitance channel image, which reveals variations at the mV scale. (c) Line profile illustrating the capacitance information.

## References

- [1] ScanWave Primenano: <https://primenano.com/index.html>
- [2] Park Systems Corp. (2022). PinPoint Nanomechanical mode. Suwon, South Korea: <https://www.parksystems.com/index.php/park-spm-modes/97-mechanical-properties/3601-pinpoint-nanomechanical-mode>
- [3] Park Systems Inc (2021). Accurate dopant profiles of semiconductor device structures with QuickStep. California, USA.: <https://www.parksystems.com/applications/electrical-electronics/semiconductor/387-accurate-dopant-profiles-of-semiconductor-device-structures-with-quickstep-scanning-capacitance-microscopy?highlight=WyJxdWlja3-N0ZXAiLIncXVpY2tdGVwJyJd>
- [4] ScanWave Pro Solutions. California, USA.: <https://primenano.com/new!-scanwave-pro%e2%84%a2-solution.html>
- [5] Park SmartScan: Park AFM Operating Software <https://parksystems.com/products/operating-software/park-smartscan>
- [6] Proceedings Volume 11611, Metrology, Inspection, and Process Control for Semiconductor Manufacturing XXXV; 116110K (2021): <https://doi.org/10.1117/12.2584560>.

# PRIMER: SURFACE ANALYSIS TECHNIQUES USING ATOMIC FORCE MICROSCOPY

Chie Goto, Jong Deok Kim, Park Systems Japan

## Introduction

Atomic force microscopy (AFM) is a nano-scale microscopy technology that employs a sharp cantilever featuring a probe tip with a width less than 10 nm. By gauging the displacement of this cantilever, AFM detects atomic forces – both attraction and repulsion – occurring between the probe tip and the sample surface. A super luminescent diode (SLD) light source is utilized to monitor the cantilever's displacement (refer to Figure 1). The motions of the sample and cantilever in the X, Y, and Z directions are controlled by piezoelectric scanners. Through these mechanisms, precise three-dimensional topography data of the sample surface can be captured. This topography data forms the basis for various applications, with specific measurement modes chosen depending on the application's requirements.

The evolution of AFM is underpinned by the integration of three distinct application techniques, each contributing to high-resolution three-dimensional topography quantification. technique A involves surface scanning using a probe, enabling simultaneous measurement of mechanical, electrical, and chemical properties at the same locations on the sample. technique B, on the other hand, doesn't require scanning; it involves moving the Z axis of the scanner to make the probe "contact and separate" from the sample. The force/distance curve plotted from cantilever deflection and deformation during this process quantitatively determines the interaction force between the probe and the sample. Lastly, technique C employs the probe for tasks such as indentation, scratch tests, and wear tests on the sample surface. Additionally, it serves as a tool for mechanical processing, anodization-based surface patterning, and mechanical property assessment, distinct from the usage scenario of technique B.



Figure 1. The tip scans the sample surface, and the SLD is used to detect the displacement of the cantilever caused by the change in surface height.

## Technique A: Property Mapping

This is an example that shows the topography, surface potential, and magnetic force of a two-phase stainless steel with Austenite and Ferrite organizations that are coexisting [1]. The scan size is 20  $\mu\text{m}$  x 20  $\mu\text{m}$ , and the magnetic film was coated with a probe to measure the topography information, electrical information, and magnetic information simultaneously.

The topography information of the polished sample surface

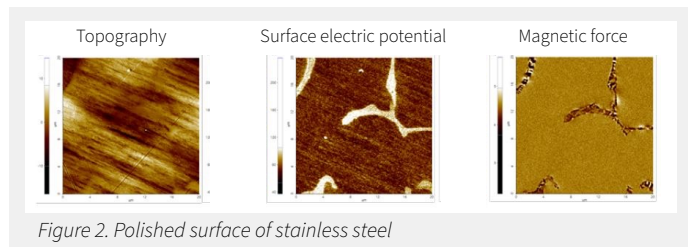


Figure 2. Polished surface of stainless steel

was flat, and it was difficult to identify the two materials from the topography, but it was possible to identify them from the electrical and magnetic properties (Figure 2). Regarding the phase separation of the solid solution in which Ferrite was mixed to reinforce the stress corrosion cracking, which is a disadvantage of the Austenite system, the Ferrite phase has a strong magnetism. This can be seen as a striped pattern when viewed with a Magnetic force microscope (MFM). The paramagnetic Austenite phase, however, is uniform. The Kelvin probe force microscope (KPFM) can measure the difference in work function between the two materials. This is done by measuring the contact potential difference between the conductive probe and the sample surface.

The KPFM image shows that the surface potential of the Ferrite phase is higher than that of the Austenite phase.

## Technique B: Nanomechanical Characterization

First, we introduce the evaluation of elasticity, adhesion, and deformation by PinPoint nanomechanical mode. When obtaining the force/distance curve, quantitative measurement of local elasticity, adhesion, and deformation can be performed if the spring constant of the cantilever is pre-calibrated. There is a method called PinPoint nanomechanical mode [2]. (Figure 3) to obtain the force/distance curve for each data point in the scan area, which is often used for evaluation of the dissolved membrane.

By considering the force/distance curve obtained and the amount of pressing to the sample of cantilever, the mechanical properties such as Young's modulus, deformation amount, adhesion force and hardness can be quantitatively calculated from the force/separation curve as shown in Figure 4. As an example of membrane measurement, the results obtained by PinPoint nanomechanical mode for polished surface PS-PVAc film, which is widely used for coating material and packaging material, are shown. Clear phase separation of polyvinyl acetate (PVAc) in the matrix part (sea) and polystyrene (PS) island is observed. It indicates that PS is harder than matrix PVAc, and it has a large adhesive force, a small amount of deformation, and a high elastic modulus.

Moving on, we delve into the assessment of friction forces through the utilization of the Lateral force microscope (LFM). The

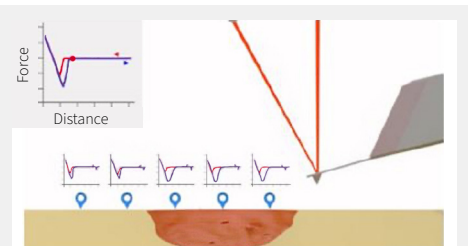


Figure 3. PinPoint nanomechanical mode. Obtain the force/distance curve at each data point. Different parts of the material change the topography of the force/distance curve.

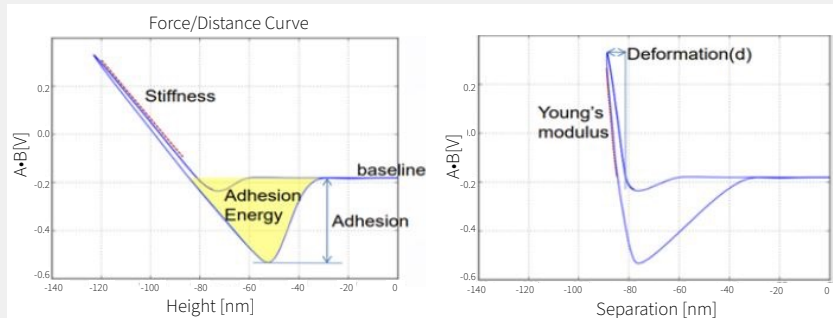


Figure 4. Force/Distance Curve

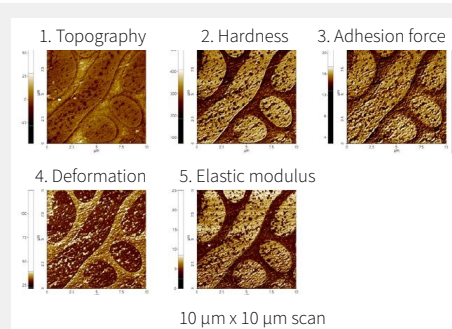


Figure 5. Simultaneous evaluation of mechanical properties at the same location as the topography image on the upper left

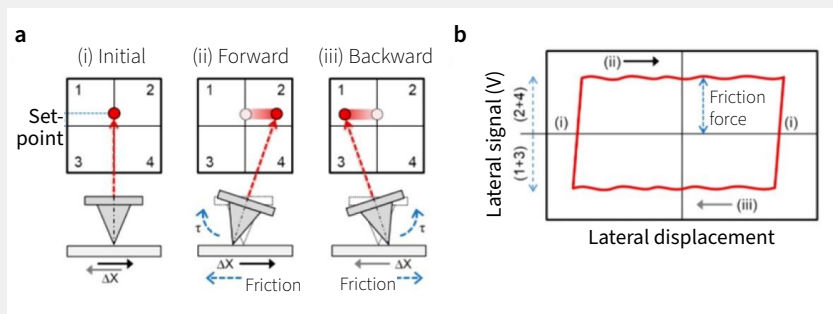


Figure 6. (a) Capturing displacement caused by scan direction and cantilever twist as lateral changes in the photodetector, (b) formation of a friction loop through the reversal of forward and backward scans.

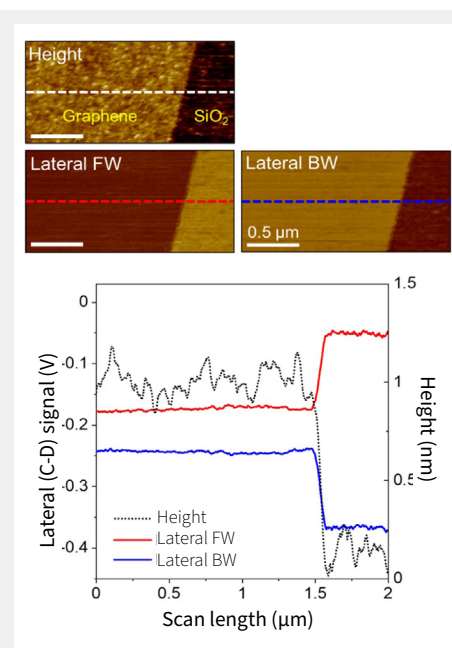


Figure 7 shows the results of scanning two materials across each other on a silicon substrate with flake-topography graphene deposited on it, resulting in a friction loop with the horizontal forward and backward scans reversed. The cantilever was previously used to calculate the sensitivity in the lateral direction by AFM thermal seeder method. From these results, as shown in Figure 8, a lateral force of about 13.7 nN was calculated for SiO<sub>2</sub> on the silicon substrate and 2.9 nN for the graphene part [3].

LFM serves as a quantitative tool for evaluating the frictional behavior of materials. It achieves this by detecting the torsion of the cantilever in the lateral direction, which is influenced by the elasticity, adhesion, and deformation calculated from the vertical displacement of the cantilever. This lateral displacement, induced by friction, results in the formation of a friction loop, as depicted in Figure 6(b). This loop emerges during both the forward and backward scans, encompassing one complete round trip.

### Technique C: Thin Film Characterization and Nanofabrication

Incorporating Contact mode AFM, which maintains continuous contact between the cantilever tip and the sample, offers a novel avenue for assessing the mechanical properties of thin films and enabling atomic-order processing technologies that were previously challenging to appraise.

In the realm of material strength, assessing mechanical properties at the nano to micro scale is crucial, as seen in the case of diamond-like carbon (DLC) films. DLC, an amorphous carbon film with properties akin to diamond, boasts high density and quasi-stability. Fine-tuning its nanostructure further enhances its tribological properties. Nano-composite techniques involving diverse materials have been widely employed to enhance surface mechanical properties. The utility of AFM nanoindentation and nano-scratch in evaluating these nanoscale features is well-recognized.

To enhance carbon film strength, elements like boron (B) and nitrogen (N), which form strong bonds with carbon (C), come into play. Nano-periodic lamination involves stacking different materials alternately at the nanometer scale, resulting in energy changes within the film due to its nano-periodic structure. This design leads to improved properties like elasticity and hardness more than the single films of the constituent materials stacked individually (Figure 9).

During nanoindentation using a diamond probe with varying nano-periods (2, 4, 6, 8, and 10 nm), the 4 nm-period film emerged as the hardest (Figure 10). Moreover, the laminated film exhibited greater hardness than the individual C and BN films.

The laminated film's outstanding tribology characteristics make it versatile as a thin film, with potential applications in various areas. For instance, it can serve as an AFM high-density recording medium. Leveraging the laminated film, precise

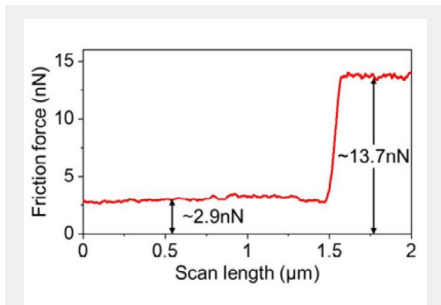


Figure 8. Cross-sectional profile of LFM (lateral force microscopy) image

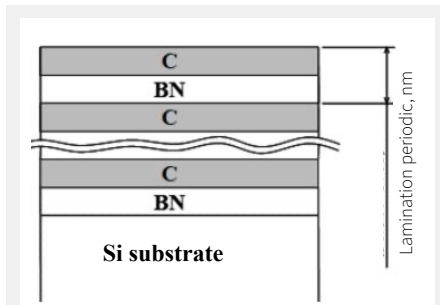


Figure 9. Model of C/BN nano-periodic multilayer film

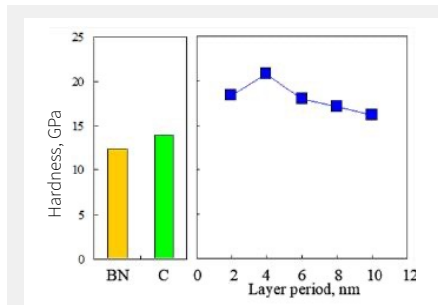


Figure 10. Nanoindentation hardness of C/BN laminated film

layer-by-layer removal can be achieved, enabling accurate processing to a specific depth.

Figures 11 and 12 illustrate step groove processing using a C/BN 2 nm periodic laminated film, designed for multi-value recording at the same location. The processing parameters involve a 200 nm processing length and a 100 nm line interval. The initial processing depth was 1 nm, increasing by 1 nm with each subsequent process, culminating in 5 nm for the fifth iteration. This demonstrates the adjustability of the processing depth based on the number of processing cycles.

Moving forward, we explore an instance of silicon nanomachining. Employing atomic-order processing, nanolithography is harnessed to create nanomachines and nanodevices [6]. An additional advantage of this method is that the machined topography can be measured at the nanometer scale using the same chip post-nanomachining.

Figure 13 shows an example of the nano rise topography formed by the AFM. The load was increased from 10  $\mu\text{N}$  in the upper right to 10  $\mu\text{N}$  each, 20  $\mu\text{N}$ , 30  $\mu\text{N}$  in the center, and to 90  $\mu\text{N}$  in the lower left. Although the height of the bumps increases with the load, the bumps [7] have almost the same shape.

The observed bulging phenomenon is attributed to the friction of the diamond indenter, causing bond breakage at areas of maximum shear or tensile stress within the silicon. These areas react with water or oxygen from the surface and surroundings to form silicon oxide and silicon hydroxide [8,9].

## Conclusion

Atomic Force Microscopy (AFM) has revolutionized the realm of nanoscale analysis through its versatile techniques. Technique A, focused on Property Mapping, enables the simultaneous

evaluation of topography, surface potential, and magnetic force of complex materials, shedding light on intricate material characteristics that would be difficult to discern through topography alone. Technique B, nanomechanical characterization, empowers precise assessment of elasticity, adhesion, and deformation through the innovative PinPoint nanomechanical mode. This technique offers a comprehensive understanding of materials' mechanical properties, aiding advancements in material science. Technique C, thin film characterization and nanofabrication, propels thin film analysis to new heights, revealing novel insights into mechanical properties and paving the way for atomic-level processing techniques. Collectively, these techniques broaden our horizons in material research, offering unprecedented insights into the atomic world and sparking transformative possibilities in fields ranging from electronics to materials engineering. The dynamic synergy of these techniques positions AFM as an invaluable tool driving innovation and discovery across diverse scientific domains.

## References

- [1] Sample courtesy: Hyun-Bae Lee, Nuclear & Quantum Engineering, KAIST, Korea
- [2] Park Systems Introduces PinPoint™ Nanomechanical Mode to Characterize Nano Mechanical Properties of Materials and Biological Cells. Available from: <http://www.parkafm.com/index.php/company/news/press-release/450-nanomechanical>
- [3] Research Application Technology Center, Park Systems Corp: Quantitative frictional properties measurement using atomic force microscopy (2021)
- [4] 三宅正二郎, 関根幸男, 金 鍾得, 山本洋和, ナノ周期積層膜の摩擦特性を活用したナノ加工技術の開発, 精密工学会誌, 66, 12 (2000) 1958
- [5] Shojiro MIYAKE and Jongduk KIM, "Nanoprocessing of Carbon and Boron Nitride Nanoperiod Multilayer Films", Jpn. J. Appl. Phys. Vol. 42 (2003) pp. L 322-L 325.
- [6] 金 鍾得, 三宅正二郎, メカノケミカル反応によるシリコンのナノメータ隆起・除去加工とそのエッチングマスクへの応用, 精密工学会誌, 68, 5 (2002) 695
- [7] Shojiro Miyake, Mei Wang and Jongduk Kim "Silicon Nanofabrication by Atomic Force Microscopy-Based Mechanical Processing", Journal of Nanotechnology 2014 1-19
- [8] Shojiro Miyake and Jongduk Kim, "Increase and decrease of etching rate of silicon due to diamond tip sliding by changing scanning density", Japanese Journal of Applied Physics, vol. 41, no. 10, pp. L1116-L1119, 2002
- [9] Shojiro Miyake and Jongduk Kim, "Nanoprocessing of silicon by mechanochemical reaction using atomic force microscopy and additional potassium hydroxide solution etching", Nanotechnology, vol. 16, no. 1, pp. 149-157, 2005.

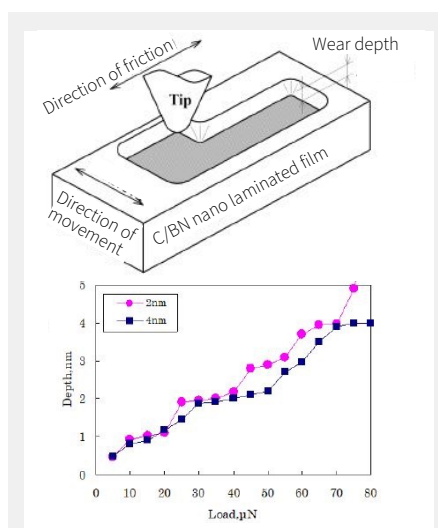


Figure 11. Micro-abrasion characteristics of C/BN laminated film by AFM

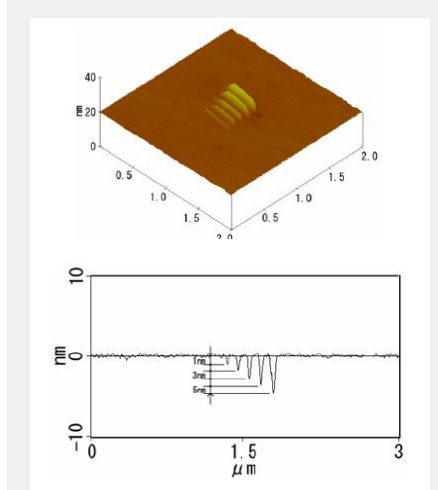


Figure 12. Stepped groove processing of laminated film

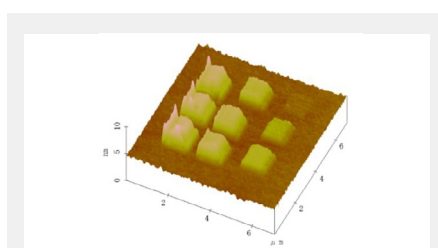
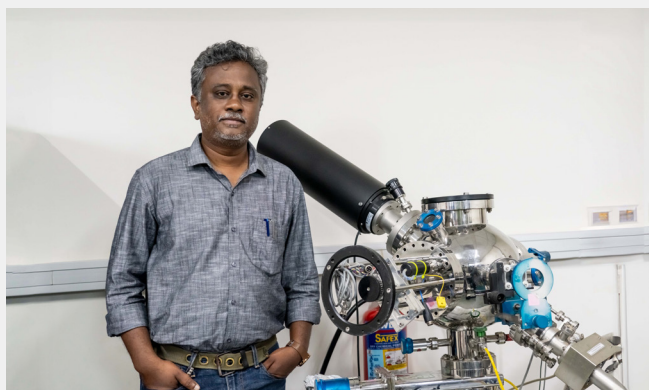


Figure 13. Raised silicon

# NANOSCIENTIFIC MAGAZINE INTERVIEW

**Ranjith Ramadurai**  
Professor at Indian Institute of Technology Hyderabad,  
Medak, Telangana, India



## About the Professor

Professor Ranjith Ramadurai, a leading nanotechnology expert, has dedicated over two decades to teaching and researching at the Indian Institute of Technology Hyderabad (IITH). His work encompasses atomic force microscopy (AFM), nanoscale characterization, and materials science, with 70+ papers in peer-reviewed journals and accolades like the Young Scientist Award from the Department of Atomic energy and young researcher award from Materials Research Society of India (MRSI). Besides teaching a range of courses at IIT Hyderabad, including AFM, nanoscale characterization, and materials science, Professor Ramadurai, an esteemed figure in the nanotechnology realm, serves on journal editorial boards, speaks at global conferences and establishing Nano materials for smart materials and devices lab at IIT Hyderabad, contributing significantly to global nanoscience.

**NS:** Can you briefly describe your nanoscience and nanotechnology journey and what first ignited your interest in this field?

### Ramadurai:

I began my Ph.D. research at the Indian Institute of Science, Bangalore, focusing on the growth of multifunctional oxide superlattice structures and studying their interfacial influences. My work encompassed exploring interfacial coupling in various superlattices and examining strain impact on ferroelectric domains using piezo-force microscopy. Fascinated by nanotechnology, I employed AFM to image nanostructure nucleation sites and utilized PFM and EFM imaging modes. During my postdoctoral fellowship at CRISMAT, ENSICAEN, France, I expanded my focus to fabricating epitaxial nanostructures and employed piezoresonance force microscopy for imaging.

Later, as an Alexander Von Humboldt fellow at Leibniz University of Hannover for two years, I contributed to a project on developing resonant tunnel diode structures with high-k dielectric tunnel barriers. I then pivoted to studying smart materials from multifunctional oxides and nanostructures. Now, at IIT Hyderabad, our lab is centered on researching smart materials and nanoscale devices, focusing on in-situ piezoresonance force imaging of nanostructures.

**NS:** How has AFM technology, a key focus of your research,

evolved over time and what developments are you currently exploring?

### Ramadurai:

AFM's evolution from a morphology imaging system to featuring various functional imaging modes has always intrigued me. Our lab at the Indian Institute of Science, Bangalore, housed the first AFM, allowing me to study the nucleation sites of thin films at early growth stages, a challenge I had faced earlier. The introduction of integrated imaging modes like magnetic force and piezoresonance force imaging has made functional domain imaging at the nanoscale possible. Currently, our group is focused on exploring advanced features like imaging surface potentials and mapping force-displacement curves at hybrid material interfaces.

**NS:** Can you share the areas of nanoscale characterization your research group is focusing on?

### Ramadurai:

The research group is now concentrating on imaging functional domains under live conditions, utilizing scanning probe microscopy with in-situ sample stages for imaging amidst various fields and stresses. The primary focus is on the electric and magnetic order of nanomaterials under multiple thermodynamic parameters and analyzing functionalities at the interfaces of hybrid nanocomposites for energy harvesting.

**NS:** Your research has resulted in numerous publications. Could you discuss some of your most significant findings or contributions to the field?

### Ramadurai:

In the early 2006-2008 period, strain engineering was pivotal in studying multiferroics, especially BiFeO<sub>3</sub> (BFO), a prominent room-temperature multiferroic. Our focus was on strain-induced polarization constraints in BFO-based epitaxial superlattices. Using strain engineering and piezoresonance force microscopy, we demonstrated the suppression of specific polarization variants and associated structural transformation in BFO (Ranjith.R et al, APL 96(2010)).

We used strain engineering in BFO epilayers to induce multiphases akin to a morphotropic phase boundary, previously attainable only through compositional variation. This method enhanced the piezoelectric behavior of mixed-phase epilayers, showing a 200% improvement compared to single-phase epilayers (Sajmohan MM et al, JAP 125 (2019)).

Using a piezoresonance force microscope and a specialized X-ray analysis method, we identified the size of strain gradients in nanocomposites, enabling us to attain desired properties in a magnetoelectric composite (Anantha P Bhat et al, ACS Appl. Nano. Mater (2022)).

**NS:** Can you outline the challenges and opportunities in nanotechnology today, particularly in India?



**Ramadurai:**

Nanotechnology in India is ripe with opportunities, thanks to supportive government policies and the India Semiconductor Mission. These not only bolster the traditional electronic industry but also encourage innovations in non-conventional fields like sensors and piezoelectrics that don't demand extensive infrastructure. Startups focusing on nano-devices in sectors like environmental, clean water, and healthcare are pivotal for economic growth. Young researchers are urged to address local challenges through nanotechnology, promising a bright future for the country.

**NS:** What advice would you give to aspiring nanoscientists and researchers starting their careers?

**Ramadurai:**

I've discussed nanotechnology's scope in India, but it's a fascinating field globally, with diverse opportunities for interdisciplinary experts. Anyone, regardless of their undergraduate training or degree, can find a nanotechnology aspect aligning with their interests. STEM education is not only engaging but also crucial as the world faces sustainable development challenges requiring specialized knowledge in different nanotechnology areas. So, honing a specific skill set is imperative.

**NS:** Beyond research and teaching, what hobbies or interests keep you balanced and motivated?

**Ramadurai:**

Though teaching and research never bore me, two of my major

interests outside of these are music, primarily classical Indian flute, and playing soccer. In fact, I hold the record for being the first goal scorer in our institute faculty soccer team during the inter-IIT tournament, a record I believe no one can alter in the history of IIT Hyderabad.

**NS:** Can you share any exciting upcoming projects or collaborations with our readers?

**Ramadurai:**

Currently, we are working on a theoretical and experimental combination of mechanically induced electric polarization rotation and the functional domains in and around defective regions of epilayers. We hope that this research will provide significant insights into the material. It involves a combination of theory and experiments, focusing on stress-induced polarization rotation, utilizing a sample stage specifically designed for AFM studies.

**NS:** What message do you have for the scientific community, particularly young aspirants in nanoscience and technology?

**Ramadurai:**

To the younger generation, and to some extent, the older generation, I would like to say that science and technology have evolved to a stage where a rigid thought process constrained by disciplinary boundaries no longer holds relevance. We are at a stage where we need to think beyond and across disciplines to work towards a sustainable global future. To be more specific, for the younger generation, I would like to say: be open and stay passionate.

**About the University**

Founded in 2008, the Indian Institute of Technology, Hyderabad is a prestigious public technical and research university known for its diverse academic programs and excellence in teaching and research. Located in Telangana, India, it ranks among the country's top engineering institutes and is celebrated for national and international research collaborations, especially in nanotechnology. IIT Hyderabad, ranked #3 nationally for innovation, is home to the advanced Nano-X Research lab, specializing in nanoscale characterization, materials science, and bioengineering through atomic force microscopy.

# DYNAMIC SELF-STABILIZATION IN THE ELECTRONIC AND NANOMECHANICAL PROPERTIES OF AN ORGANIC POLYMER SEMICONDUCTOR

Illia Dobryden<sup>1,2,8</sup>, Vladimir V. Korolkov<sup>3,8</sup>, Vincent Lemaur<sup>4</sup>, Matthew Waldrip<sup>5</sup>, Hio-leng Un<sup>6</sup>, Dimitrios Simatos<sup>6</sup>, Leszek J. Spalek<sup>6</sup>, Oana D. Jurchescu<sup>5</sup>, Yoann Olivier<sup>7</sup>, Per M. Claesson<sup>1</sup> & Deepak Venkateshvaran<sup>6</sup>

<sup>1</sup> KTH Royal Institute of Technology, Sweden. <sup>2</sup> Luleå University of Technology, Sweden. <sup>3</sup> Park Systems UK Limited, UK. <sup>4</sup> University of Mons, Belgium. <sup>5</sup> Wake Forest University, NC, USA. <sup>6</sup> University of Cambridge, UK. <sup>7</sup> Université de Namur, Belgium. <sup>8</sup> These authors contributed equally: Illia Dobryden, Vladimir V. Korolkov.

*This article has been condensed by NanoScientific under a Creative Commons Attribution 4.0 International License for the purpose of providing shorter and more accessible reading. For the full original article, please go to <https://doi.org/10.1038/s41467-022-30801-x> [www.nature.com/naturecommunications](http://www.nature.com/naturecommunications).*

## Abstract

The field of organic electronics benefits from new conjugated semi-conducting polymers with resilient molecular backbones and high charge carrier mobilities. Indacenodithiophene-co-benzothiadiazole, previously thought to lack microstructural order, exhibits nanosized domains of high order in its thin films. Its high-performance electrical and thermoelectric properties stabilize rapidly after air exposure, while nanomechanical properties equilibrate over longer timescales due to solvent molecules' gradual release from the surface. This study sheds light on the dynamic evolution and stability of this prototypical organic semiconductor's device properties.

## Introduction

Organic semiconducting polymers based on donor-acceptor motifs have gained prominence in organic electronics due to their high charge carrier mobilities, sometimes exceeding 1 cm<sup>2</sup>/Vs, and their ability to transport both negatively charged electrons and positively charged holes. Among these, a notable subset consists of polymers with a planar backbone as the donor segment, limiting torsion within the molecule. An exemplary polymer demonstrating this sought-after molecular arrangement is indacenodithiophene-co-benzothiadiazole (C16-IDTBT), known for its efficient charge carrier transport along its backbone. In this study, nanoscale regions of high ordering (~15 nm) within device-grade thin films of C16-IDTBT are conclusively shown, enhancing our understanding of its charge transport properties.

Previously investigated through field-effect transistor and Seebeck coefficient measurements, C16-IDTBT displays low torsional disorder and favorable charge transport characteristics. However, this study sheds light on a previously overlooked aspect of C16-IDTBT's behavior. The device characteristics of C16-IDTBT rapidly improve towards ideality during the hours following fabrication and upon exposure to ambient conditions. While efforts have been made to stabilize trap-free hole transport in C16-IDTBT devices using additives,

this study demonstrates how self-induced stabilization can occur over time under ambient conditions alone. Additionally, nanomechanical properties of the polymer stabilize with time, displaying texture due to the gradual removal of residual low molecular weight additive solvent molecules from the polymer film.

Understanding the complete electrical, thermoelectric, and nanomechanical properties of C16-IDTBT, as well as their time evolution, is crucial for its application in next-generation air-stable polymer semiconductor-based electromechanical devices. This research highlights the significance of strictly connecting measured properties to ambient conditions under which they are reported as organic materials often exhibit dynamic evolution. It also emphasizes the importance of reporting all fabrication and characterization procedures to ensure better reproducibility between different labs, advancing the field of organic electronics.

## Results and discussion

This research utilizing high-resolution transmission electron microscopy (TEM) has presented compelling evidence of nanoscale order within C16-IDTBT thin films, contradicting previous assumptions about their largely amorphous microstructure. Preserving the pristine large-area structural integrity of these thin films, the atomic force microscopy (AFM) was employed to observe minute regions with aligned polymer filaments, unveiling a nanoscale periodicity of 1.6 nm. The nanoscale order confirmed earlier findings from high-resolution TEM and scanning tunneling microscopy (STM), highlighting a liquid crystalline-like character with aligned polymer backbones. This study serves as an essential demonstration that simple sample preparation techniques can facilitate the observation of nanoscale ordering in C16-IDTBT thin films.

Figure 1(a) shows the chemical structure of C16-IDTBT, a copolymer of indacenodithiophene (IDT) and benzothiadiazole (BT) units. Figures 1(b) and (c) display height topography and phase contrast images obtained with an atomic force microscope (AFM) on a stabilized thin film of C16-IDTBT. Aligned polymer filaments are observed at this resolution. A high-resolution image (Fig. 1(d)) shows two regions within 30 nm of each other; one with significant order and the other with unclear ordering. The high-order region exhibits bright streaks corresponding to individual polymer backbones. The thin film's molecular backbone faces down on the substrate, with  $\pi$ - $\pi$  stacking perpendicular to the substrate. AFM scans reveal a periodicity of 1.6 nm in the ordered region (Fig. 1(e)). This periodicity does not confirm STM findings of sidechain

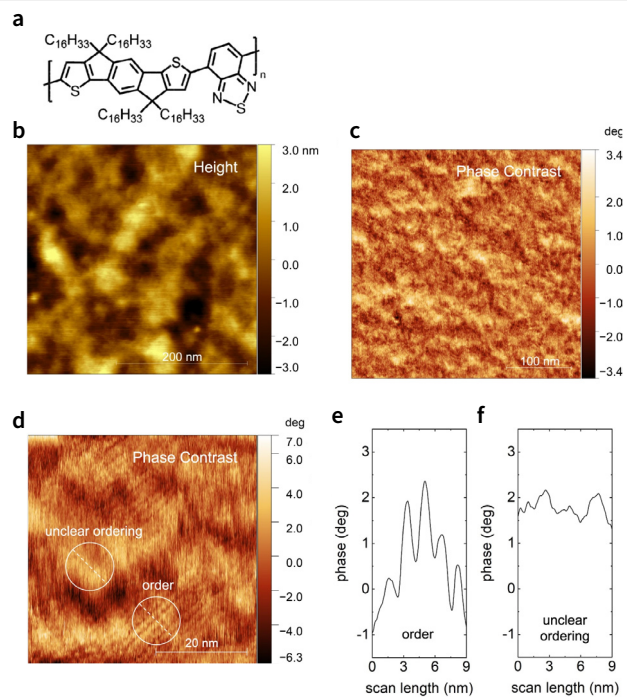


**Fig. 1** Nanostructure of C16-IDTBT films. (a) Chemical structure of a C16-IDTBT monomer showing its fused donor molecular unit (IDT) and its acceptor molecular unit (BT). (b) Height topography of a C16-IDTBT spin-coated thin film. (c) Corresponding phase contrast image of the C16-IDTBT thin film on the scale of hundreds of nanometers. (d) Phase contrast image on the scale of tens of nanometers demonstrating regions of order 10–15 nm across and regions of unclar ordering within tens of nanometers from the ordered regions. (e) Line scan along the dashed straight lines of (d) in the ordered region. (f) Line scan along the dashed straight line of (d) in the region of unclar order. The distance between the parallel polymer backbone filaments of (d) is ~1.6 nm and is smaller than that expected for in-plane sidechain interdigitation.

interdigitation in dispersed C16-IDTBT molecules. However, it aligns with recent TEM investigations, showing a liquid crystalline-like character without interdigitation of alkyl side chains in the film. Polymer backbones are parallel with their molecular faces looking up, and the bright regions are attributed to non-planar  $sp^3$  bridging carbons in the IDT units (Fig. 1(f)). These AFM results confirm the observed length scale of order and the parallel polymer backbone arrangement seen in high-resolution TEM and STM studies. Notably, the 50 nm thick films were spin-coated with common parameters used for C16-IDTBT-based organic transistors, requiring simple sample preparation.

A study was conducted to investigate how the electrical and thermoelectric properties of C16-IDTBT-based devices evolve over time. This organic semiconductor is known for its high charge carrier mobilities. Both organic thin-film transistor characteristics and the gate voltage modulated Seebeck coefficient were measured within the same device during the study. The results showed a remarkable improvement in the electrical behavior of the device when exposed to ambient air. The on-current increased significantly, and the subthreshold swing reduced to a remarkably low value, indicating improved charge transport efficiency. After a month of air exposure, the device exhibited textbook-like output characteristics, while devices stored in a nitrogen glovebox continued to display non-ideal behavior. This enhancement was attributed to a p-doping/electron-trapping mechanism involving oxygen,

which increased the hole carrier concentration and improved charge extraction and injection.

The study also investigated the Seebeck coefficient as a measure of entropy per unit charge in the device and its relation to ambient air exposure. The reduction of the Seebeck coefficient over time suggested an increasing number of carriers participating in energy and entropy transport. Initially, the device contained more carriers in trap states that did not contribute to entropy transport at low carrier accumulation. The most rapid changes in the Seebeck coefficient occurred within the first 24 hours of air exposure, followed by gradual changes. The researchers speculated that a structural reorganization within the film, caused by the release of residual solvent over time, might accompany this behavior. These findings provide insights into the dynamic evolution of C16-IDTBT-based devices and emphasize the importance of ambient conditions in determining their electrical and thermoelectric properties.

Figure 2 and Figure 3 depict the temporal evolution of electrical and thermoelectric properties in C16-IDTBT based devices. In the case of Figure 2, measurements using organic thin-film transistors and gate voltage modulation revealed rapid enhancement of the device's electrical characteristics within the initial hours of air exposure, accompanied by significant changes in the Seebeck coefficient. This improvement is attributed to ambient air and is believed to involve a p-doping/electron-trapping mechanism mediated by oxygen. Similarly, Figure 3 illustrates that upon exposure to ambient air, C16-IDTBT devices exhibited swift enhancements, indicating reduced contact resistance and improved carrier injection and extraction. Over time, non-idealities in transistor output characteristics disappeared, possibly due to induced carriers filling traps and enhancing charge transport. The Seebeck coefficient exhibited two linear regimes, initially reducing rapidly and then gradually over time, while hole mobility initially increased and later stabilized. Notably, the relationship between the Seebeck coefficient and saturation mobility appeared linear, with both transport coefficients showing an exponential dependence on time.

The study also examined the nanomechanical properties of C16-IDTBT thin films. Unlike electrical properties, the nanomechanical properties did not change significantly with ambient exposure but stabilized over time. Regarding its nanomechanical properties, there is no difference between the evolution of organic films stored in ambient air and organic films stored in a nitrogen glovebox. Also, in contrast to C16-IDTBT's electronic property evolution, the polymer's nanomechanical properties stabilize on a longer time scale owing to a mechanism pinned not to oxygen diffusion, but to a gradual sweating-out of residual, low molecular weight solvent molecules from the organic polymer film's surface.

Overall, the research highlights the dynamic nature of C16-IDTBT-based devices and the crucial role of ambient conditions in shaping their electrical, thermoelectric, and nanomechanical properties. The study sheds light on the complex interactions within the devices, providing valuable insights for the development of advanced polymer semiconductor-based electromechanical devices.

In addition, the study investigated the temporal evolution of

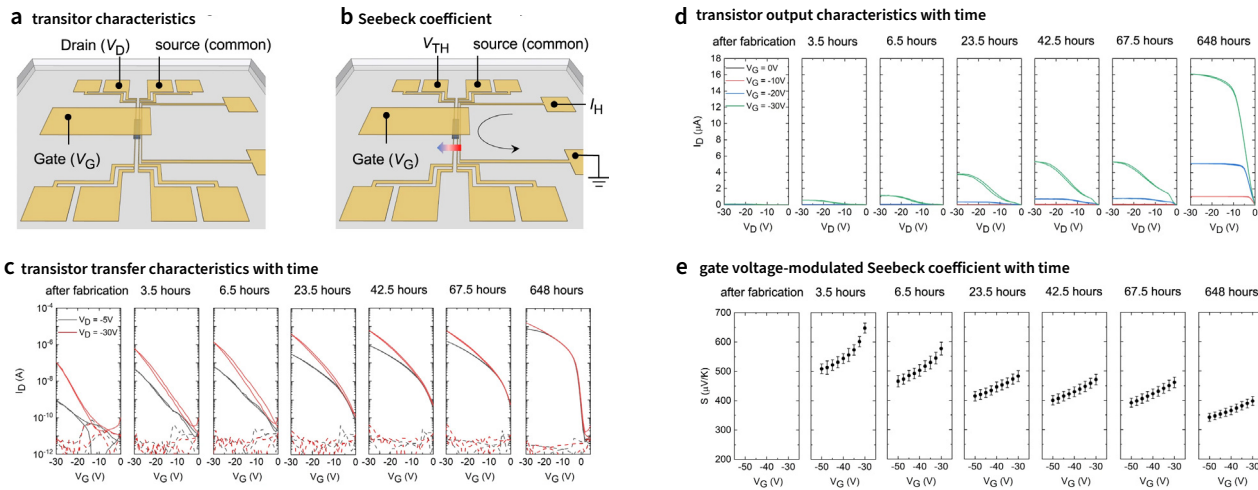


Fig. 2 Time evolution of the electrical and thermoelectric properties of C16-IDTBT. (a) Device configuration for the measurement of transistor transfer and output characteristics. (b) Device configuration for the measurement of the gate voltage modulated Seebeck coefficient. The gradient arrow indicates the direction of the positive temperature difference. (c) Transistor transfer characteristics in both the linear regime and the saturation regime over time. The dotted lines are the gate leakage currents in the dielectric. (d) Transistor output characteristics over time. (e) Gate voltage modulated Seebeck coefficient measured over time in ambient air, in which the error bars arise from the linear fit of the thermal voltage to the applied temperature differential (See Supplementary Information Section 5 in the original paper).

electrical, thermoelectric, and nanomechanical properties in C16-IDTBT thin films. The nanomechanical properties were probed using AFM to map surface topography, stiffness, adhesion, and modulus. Films exposed to ambient conditions showed improved electrical characteristics and carrier mobility over time. The Seebeck coefficient and saturation mobility demonstrated a linear relationship, indicating a new scaling law. The improvement in device characteristics was attributed to oxygen diffusion, doping, and microstructure rearrangement due to solvent removal. The nanoscale mechanical modulus exhibited texture, with nanocrystalline regions being stiffer than amorphous regions.

Furthermore, the study revealed that the nanomechanical properties of C16-IDTBT films continued to change over several weeks, with a gradual reduction in adhesion force and modulus due to solvent sweating out. This process occurred over a longer timescale than the stabilization of electronic mobility. The results underscored the importance of carefully documenting the conditions under which multifunctional properties of organic polymer devices are reported.

In summary, the research shed light on the intricate temporal dynamics of C16-IDTBT thin films, providing valuable insights into their electrical, thermoelectric, and nanomechanical behaviors. The findings contribute to the understanding of organic semiconductors and highlight the significance of environmental factors in shaping their performance characteristics.

Figure 4(a) and (b) display the nanomechanical properties of a C16-IDTBT thin film, stored in ambient conditions for several weeks to facilitate the evaporation of residual solvent molecules. Park System's PinPoint Nanomechanical measurement mode on an NX20 AFM was employed to examine the microscale topography, stiffness, adhesion, and elastic modulus. This method extracts nanomechanical properties using force curves that map tip-sample interactions. The film exhibited an average modulus around 2 GPa with homogeneity over a 5 μm x 5 μm area. Figure 4(b) portrays nanoscale

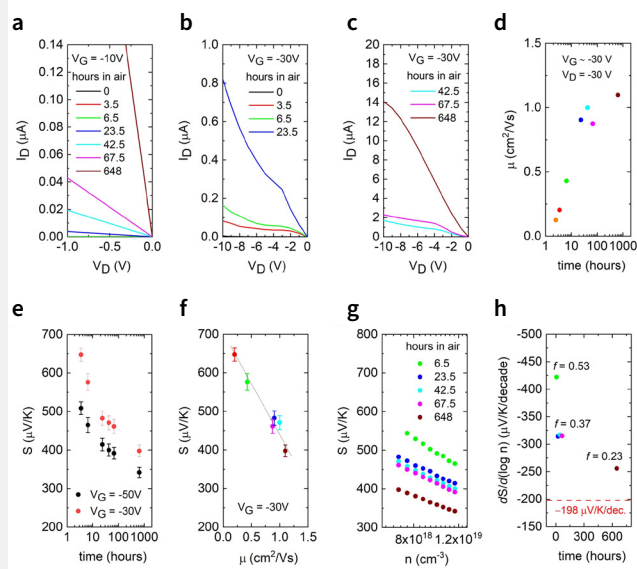
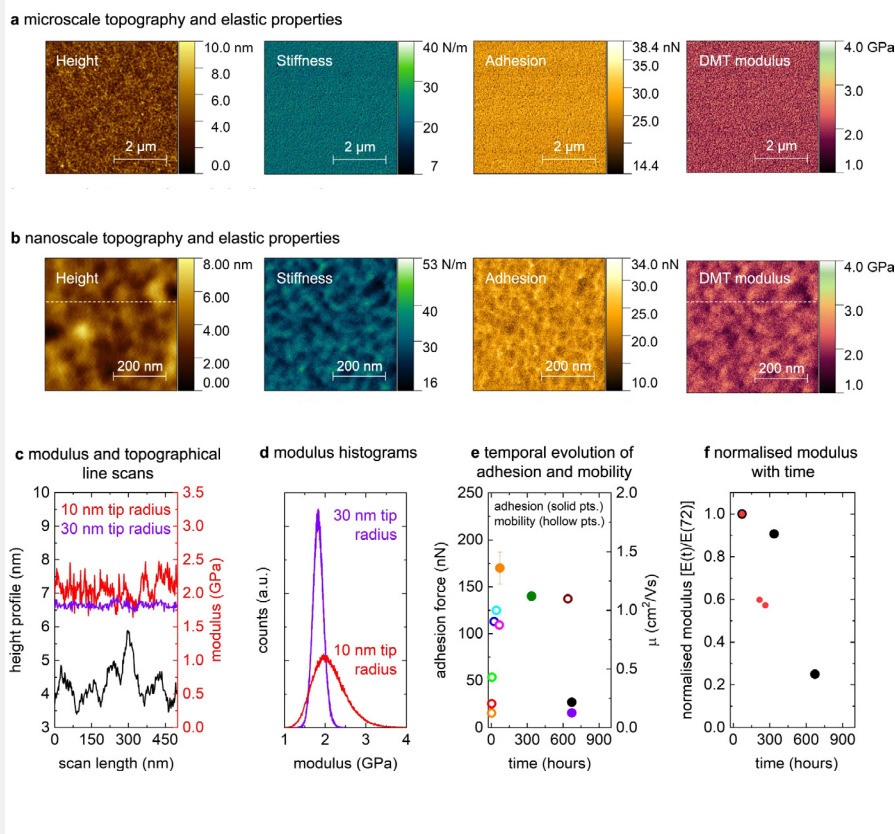


Fig. 3 Parametric dependence of mobility and Seebeck coefficient on time. (a) Output characteristics around  $V_D = 0$  V for low gate voltage of  $V_G = -10$  V. (b) Output characteristics for intermediate drain voltages  $V_D = 0$  V to  $V_D = -10$  V, high gate voltage of  $V_G = -30$  V, and for up to one day in ambient air. (c) Output characteristics for intermediate drain voltages  $V_D = 0$  V to  $V_D = -10$  V, high gate voltage of  $V_G = -30$  V, and for between 2 days and a month in ambient air. (d) Time evolution of the saturation mobility in the transistor. (e) Time evolution of the Seebeck coefficient in the transistor channel. (f) Parametric dependence of saturation mobility and Seebeck coefficient on time over three temporal decades in hours (g) Seebeck coefficient vs. carrier density in the transistor. (h) Time evolution in the slope of the Seebeck coefficient vs. carrier density in the transistor channel.

properties, showing significant texture in stiffness, adhesion, and modulus over a few hundred square nanometers. The relationship between the ordered and disordered regions was analyzed in Fig. 4(c) through line scans of topography and modulus, where texture in modulus was not influenced by tip artifact. With a 10 nm tip radius, notable features were observed on a 50 nm or smaller scale, suggesting crystallinity differences between ordered and disordered regions. However, the 30



**Fig. 4 Nanoscale mechanical properties and nanomechanical homogenization with time.** (a) Topography and elastic properties (stiffness, adhesion, and modulus) in C16-IDTBT on the microscale. (b) Topography and elastic properties (stiffness, adhesion, and modulus) in C16-IDTBT on the nanoscale. The thin films were processed under identical conditions as those used in the electrical and thermoelectric devices but were left undisturbed under ambient conditions and in the dark for several weeks to allow the low molecular weight solvent molecules to evaporate from the surface under their own volatility.

(c) Line scan of the modulus and topography along the dotted white lines shown in (b) measured using a tip radius of 10 nm. A scan of the modulus with a tip radius of 30 nm is shown in purple for comparison. (d) Comparison of modulus histograms measured with two different tip radii; a 30 nm tip radius (larger than ordered film features) and a 10 nm tip radius (equivalent or less than ordered film features). (e) Comparison showing how the film adhesion changes far slower with time than the saturation mobility. (f) Normalized modulus measured on different C16-IDTBT samples using two different AFMs. The black dots correspond to the measurements on a Park Systems NX20 and the red dots correspond to measurements on a JPK NanoWizard 3 Atomic Force Microscope. The modulus reduction and homogenization that accompanies the reduction in adhesion force takes place on a time scale longer than the stabilization of the saturation mobility.

nm tip radius produced uniform modulus readings. Figure 4(d) demonstrated histogram asymmetry, indicating potential crystallinity differences.

In contrast, a C16-IDTBT film without extended stabilization showed distinct nanomechanical properties. Over time, adhesion force and elastic modulus decreased. Initial adhesion force was high three days after film fabrication. While electronic properties stabilized within three days, adhesion gradually changed over weeks due to solvent outgassing. After a month, adhesion reached  $\sim 27$  nN, consistent with stabilized thin films and correlated with other nanomechanical measurements. Figure 4(f) illustrated a significant reduction in average modulus ( $E(t)/E(72)$ ) over time due to solvent evaporation, a process slower than hole mobility reaching its threshold value. Dynamic bubble formation was also observed on the film surface.

## Methods

### Fabrication of transistor and Seebeck devices and its measurement sequence

**Fabricating devices:** Gold electrodes micropatterned using optical lithography and thermal evaporation. A resistive stripe heater is added. Organic semiconductor C16-IDTBT overlaps the electrodes, avoiding cross talk. Organic layer 200 microns long, 1 mm wide. Source and drain electrodes double as on-chip thermometers. 500 nm Cytop-M dielectric layer processed over organic semiconductor and substrate. 25 nm gold gate electrode deposited over the dielectric, covering the organic semiconductor. Transistor characteristics and Seebeck coefficient measured with gate voltage in monitored time sequence (see Supplementary Info Section 4 in the original paper). Steps carefully executed to limit air exposure. Device measured under vacuum. Seebeck measured again after

ambient exposure. Detailed procedures in Supplementary Information.

### Pinpoint nanomechanical measurements and AFM based phase topography

Park Systems NX20 Atomic Force Microscope (Park Systems Co., Suwon, Korea) was used for both topography and nanomechanical properties measurements conducted in ambient conditions at 22°C using PinPoint nanomechanical measurements and AFM phase topography techniques. High-resolution phase maps were obtained using a novel higher eigenmode approach with Multi75Al-G cantilevers excited at the 3rd eigenmode [V. V. Korolkov et al., Nat. Commun. 10, 1537 (2019)]. Nanomechanical data was collected with PinPoint Nanomechanical mode [S. Kim et al., Nanomaterials 11(6), 1593 (2021)] on the same instrument, enabling simultaneous acquisition of topographical maps and force-distance curves at each pixel. Automated analysis provided nanomechanical properties like modulus, adhesion, deformation, stiffness, and energy dissipation. AC160TS cantilevers (Olympus, Japan) with a nominal spring constant of 42 N/m were used, calibrated before measurements. The C16-IDTBT thin film sample investigated was "stabilized," allowing solvent molecules to sweat out from its surface for reliable measurements after a few weeks.

### Data availability

The data used in this study are presented in the text and the Supplementary Information (<https://www.nature.com/articles/s41467-022-30801-x#MOESM1>). Additional data are available from the corresponding authors upon reasonable request. The Atomic Force Microscopy and Nanomechanics dataset used in Fig. 1 and Fig. 4, are available at Cambridge University's online repository: <https://doi.org/10.17863/CAM.84546>.

## PARK SYSTEMS CELEBRATES GROUNDBREAKING EXPANSION TO GWACHEON AND YONGIN 19 September 2023

Park Systems announced that it is embarking on an exciting phase of expansion. The company broke ground on its new Gwacheon headquarters on September 15, 2023, to continue its growth expanding global footprint in the coming years. "After 26 years of leasing, thanks to our accelerated growth since our KOSDAQ listing in 2015, we are proud to announce that Park Systems now has its own office building, marking a significant milestone in our journey," said Dr. Sang-il Park, Founder and CEO of Park Systems.

### Expansion to Gwacheon and Yongin

Park Systems is set to expand its headquarters and production facilities, starting with Gwacheon in 2026 and followed by Yongin in 2027. The decision to expand is driven by a substantial increase in orders due to the diversification of their industrial AFM product offerings. This expansion will enhance their production capacity and reduce dependence on core component suppliers.

### Yongin Semiconductor Cluster Allocation

In a significant development, Park Systems has secured a factory premises allocation within the SK Hynix-led Yongin Semiconductor Cluster. This strategic move positions Park Systems in a key role within this semiconductor ecosystem. The construction of the Gwacheon headquarters, representing a KRW 64.2 billion investment, begins next month and is expected to conclude by 2026, catering to the needs of a growing workforce amid business acceleration. Additionally, by 2027, Park Systems aims to occupy the Yongin production facility, spanning 13,216 square meters, in response to a surge in order volume. This comes as the company is already augmenting its production capacity by expanding leased space in Suwon.

### Diversification and Component Localization

With an annual order amount exceeding KRW 100 billion, Park Systems recognizes the need to further expand capacity beyond this level. The company has diversified its industrial AFM lineup, including extreme ultraviolet (EUV) process products. Additionally, there is a growing sentiment to internally manufacture key components as production volume increases.

### Collaboration Opportunities

Companies entering the Yongin Cluster, led SK Hynix, have the opportunity to build their factories and lease excess space to partner companies. This collaborative approach is expected to reduce production lead times and increase steady income. "We are excited to embark on this new phase of growth," said Dr. Sang-il Park. "The expansion of our headquarters is a testament to our commitment to supplying the best performing nanometrology solutions, and we are confident that it will help us achieve our goals of growth and innovation." The expansion of Park Systems represents a significant step forward in its commitment to enable nanoscience and technology advancements and providing cutting-edge solutions to its customers.



## PARK SYSTEMS RECOGNIZED IN FORBES ASIA'S BEST UNDER A BILLION 2023 18 September 2023

Park Systems announced its distinguished inclusion in Forbes Asia's "Best Under A Billion 2023." This recognition marks a second appearance for Park Systems in Forbes's prestigious list, following its remarkable inclusion in the Forbes 200 in the year 2020.

Forbes Asia's annual Best Under A Billion list is a tribute to companies that have excelled despite formidable global headwinds such as inflation and rising funding costs. In this year's distinguished list, Park Systems proudly stands as one of Korea's top 16 companies, demonstrating exceptional performance and excellence. This recognition is

especially noteworthy considering that over 20,000 publicly traded companies in the Asia-Pacific region were considered.

Park Systems is lauded for its unwavering commitment to innovation and excellence in offering pioneering solutions globally and enjoying consistent growth in revenue and earnings. The company, noted for heavy investments in R&D, has its cutting-edge nano-metrology systems, including AFMs and ellipsometers, employed across diverse industry and research sectors. Its recognition on Forbes is attributed to a meticulous evaluation process weighing financial performance, governance, and

environmental consciousness, among other criteria.

Forbes Asia's Best Under A Billion 2023 list is a testament to the resilience and success of Park Systems, and the company looks forward to further strengthening its position as a global leader in its industry.



## PARK SYSTEMS APPOINTS STEFAN SCHNEIDER AS GENERAL MANAGER OF ACCURION DIVISION 10 July 2023

Park Systems announces Stefan Schneider as the new General Manager of Park Systems Accurion Division (Park Systems GmbH), a prominent provider of imaging spectroscopic ellipsometry (ISE) and active vibration isolation (AVI) systems. Schneider brings over 11 years of experience at Accurion, specializing in R&D and product development. Schneider significantly contributed to Accurion during his tenure, leading key projects such as the development of the "UltraBAM" Brewster Angle Microscope and "EP4" Imaging Ellipsometer. He enhanced imaging optics and expanded the EP4's functionalities. Under Schneider's leadership, prototype and in-line ISE systems for memory and display inspection were successfully developed. "We are excited to announce Stefan Schneider as the new General Manager

of Accurion, Park Systems. With his extensive experience in R&D and product development, Stefan is the perfect candidate to lead Accurion into a new era of success. His strong leadership and industry expertise will drive the integration of Accurion's products with Park Systems's offerings, enhancing our capabilities in the semiconductor market." - Dr. Sang-il Park, CEO of Park Systems Corporation.

Accurion is distinguished for its expertise in ISE and AVI systems, known for advanced layer characterization and superior vibration isolation. The company's merger with Park Systems is poised to unlock new potentials, combining ISE and AFM technologies for innovative hybrid solutions. This integration strengthens their market position, while Accurion's AVI systems

enhance Park Systems's capabilities and customer reach by meeting the demand for advanced vibration isolation.

Stefan Schneider's appointment signifies an exciting chapter for Accurion, and the company looks forward to achieving new milestones under his leadership.



*A New General Manager of Park Systems GmbH Accurion Division, Stefan Schneider*

## PARK SYSTEMS INAUGURATES NEW SHANGHAI APPLICATION CENTER FOR ADVANCED NANO SCIENCE RESEARCH 15 May 2023



*Park Shanghai Application Center ribbon cutting ceremony and live demos*

Park Systems celebrated the grand opening of its new application center in Shanghai, China. The opening ceremony was held at the WE International in Shanghai, successfully witnessing the new chapter of Park Systems Shanghai Application center on May 15.

The Park Shanghai Application Center is located in the core area of Hongqiao Business District, covering a total area of nearly 500 square meters, equipped with advanced technologies to provide comprehensive technical support to customers from pre-purchase research to after-sales application needs.

The inauguration of the Park Systems Shanghai Application Center was graced by notable scientists, scholars, and corporate executives globally. Mr. Zhang Fei, the Chief Representative of Park Systems China, opened the event expressing appreciation for the attendees. Support from the Republic of Korea was affirmed by Commercial Consulate General Mr. Kim Geon-mo, who pledged assistance to Park Systems's expansion in China and commended its global standing in nano-metrology. Dr. Sang Joon Cho highlighted the center's role in advancing China's nanotechnology landscape through contributions to academic and technological development.

The inauguration of the Shanghai Application Center symbolizes a fresh chapter in academic research and industry innovation. This center is not just a research hub but also a nexus for collaborative dialogues between customers and businesses, driving advancements in nanoscience and technology. The unveiling has captured the attention of significant domestic corporations, solidifying Park Systems's leadership in the atomic force microscopy domain.

*Microscopic Thin Film Metrology and Visualization*

# Empower your research with our next-generation Imaging Ellipsometer

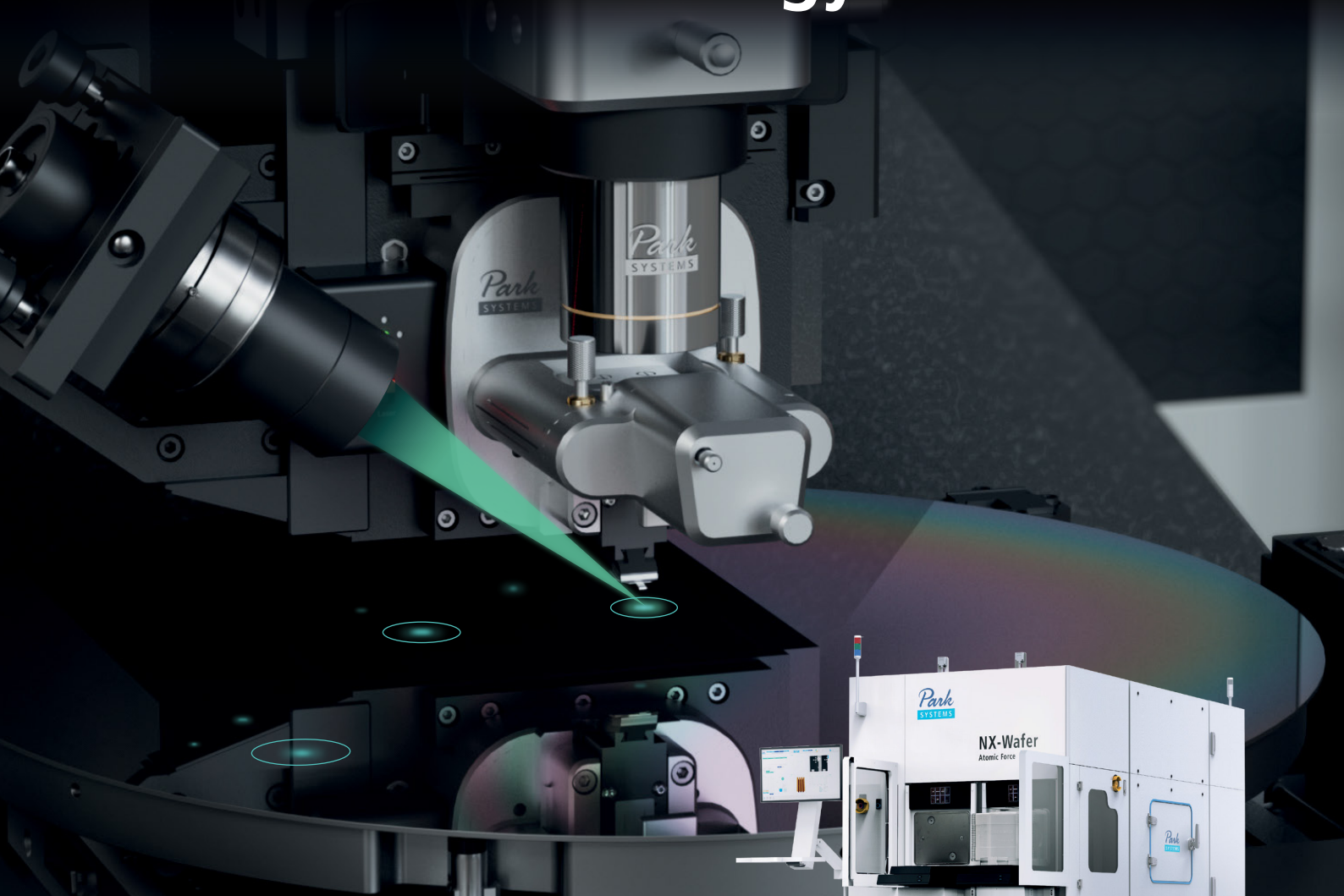


## Accurion EP4

The Accurion EP4 is our latest generation of imaging ellipsometers that combines ellipsometry and microscopy. This enables the characterization of thickness and refractive index with the sensitivity of ellipsometry on micro-structures as small as 1  $\mu\text{m}$ . The microscopic part enables a simultaneous measurement of all structures inside the field of view of the optical system.

- High lateral ellipsometric resolution for thickness and refractive index on microstructures as small as 1  $\mu\text{m}$ .
- Intuitive region selection through drawing in the live ellipsometric view before measurement.
- Continuous spectroscopic imaging ellipsometry from UV to NIR.
- Expanded application of ellipsometry to small structures with new features and accessories.

# Industry's leading automated AFM for in-line metrology solutions



## Park NX-Wafer

Park NX-Wafer is the industry's leading automated AFM metrology system for semiconductor and related fabrications. It provides wafer defect review and analysis for bare wafers and substrates, and CMP profile measurements. Park NX-Wafer has the highest nanoscale surface resolution with sub-angstrom height accuracy, scan after scan with negligible tip to tip variation and preserved tip sharpness unmatched by others.

- Low noise atomic force profiler for more accurate CMP profile measurements
- Sub-Angstrom surface roughness measurements with extreme accuracy and negligible tip-to-tip variation
- Fully automated AFM solution for defect imaging and analysis
- A fully automated system with auto tip exchange, robot wafer handler
- Capable of scanning 300 mm wafers



Watch the video

[parksystems.com/nx-wafer](https://parksystems.com/nx-wafer)

*Park*  
SYSTEMS